



# National Transportation Safety Board

Office of Aviation Safety  
Washington, D.C. 20594-2000

November 2, 2009

## **ADDENDUM 1 – METEOROLOGICAL FACTUAL REPORT**

**DCA09MA021**

### **A. ACCIDENT**

Location: Denver, Colorado

Date: December 20, 2008

Time: 1818 Mountain Standard Time (0118 UTC<sup>1</sup> December 21, 2008)

Aircraft: Continental Airlines flight 1404, Boeing 737-500, registration N18611

### **B. METEOROLOGICAL SPECIALIST**

Donald E. Eick  
Senior Meteorologist/Group Chairmen  
National Transportation Safety Board  
Operational Factors Division, AS-30  
Washington, D.C. 20594-2000

Members:

Kris Kimmons  
Systems Operations Manager  
Continental Airlines

James Sullivan  
Pilot for American Eagle Airlines  
Air Line Pilots Association

Paul Biagi  
Electronics Engineer  
Federal Aviation Administration

---

<sup>1</sup> UTC – is an abbreviation for Coordinated Universal Time.

## **C. SUMMARY**

On December 20, 2008, at 1818 mountain standard time, Continental flight 1404, a Boeing 737-500 (registration N18611), equipped with CFM56-3B1 engines, departed the left side of runway 34R during takeoff from Denver International Airport (DEN). The scheduled, domestic passenger flight, operated under the provisions of Title 14 CFR Part 121, was enroute to George Bush Intercontinental Airport (IAH), Houston, Texas. There were 37 injuries among the passengers and crew, and no fatalities. The airplane was substantially damaged and experienced post-crash fire. The weather observation in effect nearest the time of the accident was reported to be winds at 290 and 24 knots with gusts to 32 knots, visibility of 10 miles, a few clouds at 4000 feet and scattered clouds at 10,000 feet. The temperature was reported as -4 degrees Celsius.

## **D. DETAILS OF INVESTIGATION**

Additional meteorological data was collected from the National Center for Atmospheric Research (NCAR), located in Boulder, Colorado, and from additional official National Weather Service (NWS) sources including the National Climatic Data Center (NCDC). All times are mountain standard time (MST) based upon the 24 hour clock, local time is +7 hours to UTC, and UTC=Z. Directions are referenced to true north and distances in nautical miles. Heights are above mean sea level (msl) unless otherwise noted. Visibility is in statute miles and fractions of statute miles.

### **1.0 Synoptic Situation**

The synoptic or large scale migratory weather systems influencing the area were documented using standard NWS charts issued by the National Center for Environmental Prediction (NCEP) located in Camp Springs, Maryland. These are the base products used in describing weather features and in the creation of forecasts and warnings. Reference to these charts can be found in the joint NWS and Federal Aviation Administration (FAA) Advisory Circular "Aviation Weather Services", AC 00-45.

#### **1.0.1 Surface Analysis Chart**

The NWS Surface Analysis Chart for 1700 MST on December 20, 2008 (0000Z on December 21, 2008) is provided as figure 1, with the approximate location of the accident site marked by a red cross. The chart depicted a low pressure system with a central pressure of 1011-hectopascals (hPa) over the Colorado and New Mexico border, with a stationary front extending north-south across eastern Colorado, immediately east of the accident site into Wyoming turning westward

into Idaho and Oregon. A high pressure ridge<sup>2</sup> extended over Nevada, Utah into western Colorado. The pressure pattern across the Denver area resulted in a westerly winds across the Rockies.

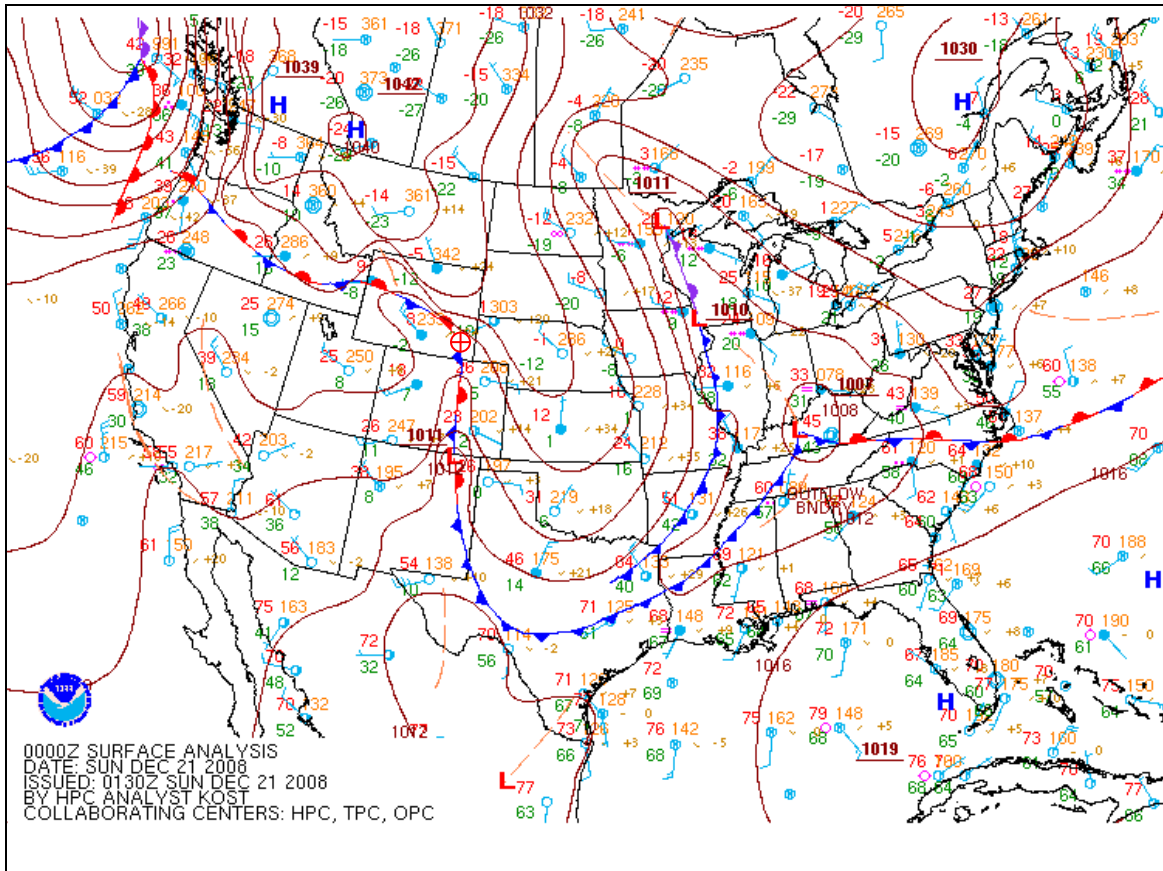


**Figure 1 – NWS Surface Analysis Chart for 1700 MST (0000Z)**

Figure 2 is the NWS Surface Analysis Chart for 2000 MST (0300Z). The chart depicted a new low pressure system in northeast Colorado at 1023-hPa immediately east-northeast of the accident site, with a high pressure system at 1031-hPa over Utah.

<sup>2</sup> Subsidence – or descending of air, which is heated by adiabatic compression is a normal characteristic of a high pressure system and a ridge. The subsidence often creates a stable layer referred to as an inversion or increase in temperature with altitude.

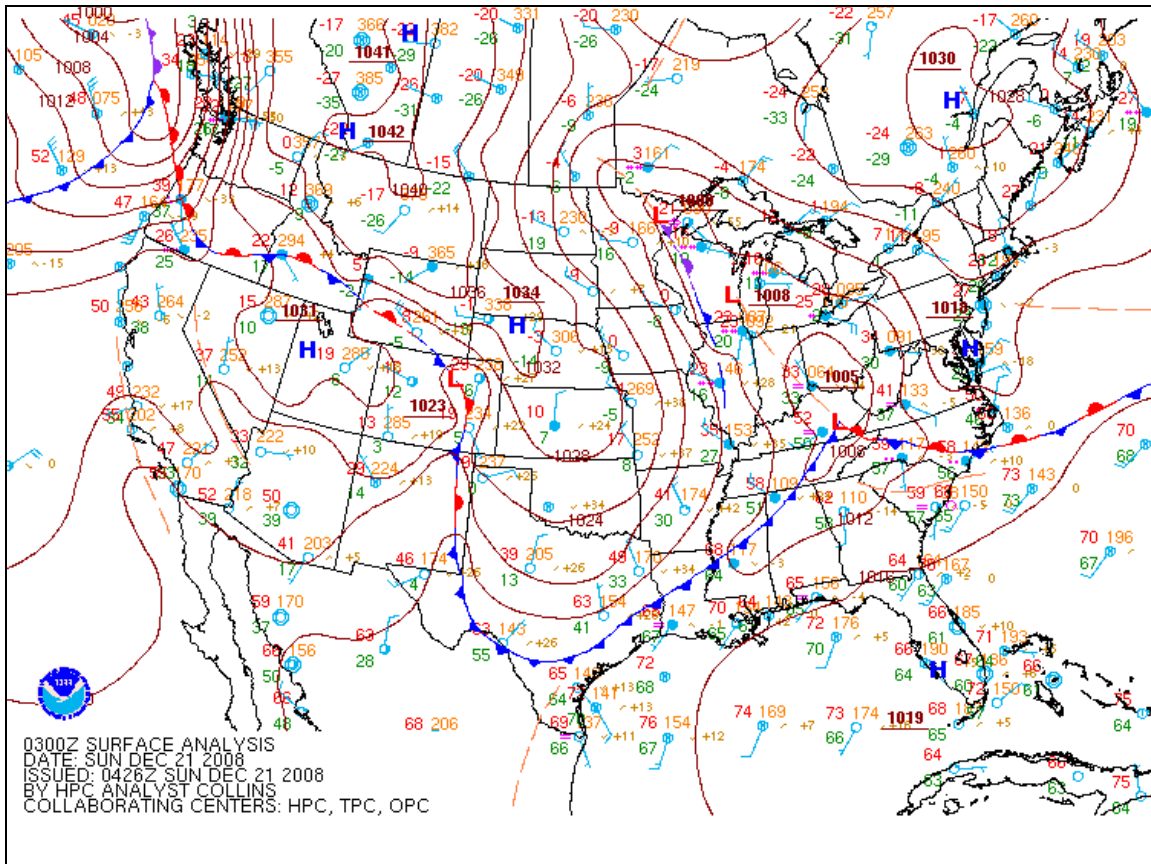


**Figure 2 – NWS Surface Analysis Chart for 2000 MST (0300Z)**

### 1.0.2 Constant Pressure Charts

Figures 3 through 6 are the NWS Constant Pressure Charts for 1700 MST (0000Z on December 21, 2008) for 700-, 500-, 300-, and 200-hPa respectively. The charts depicted west-northwest winds over Colorado with little variation in direction, with winds increase in speed with height, with a maximum wind speed of 110 knots at 30,000 feet. The maximum jet stream<sup>3</sup> wind downstream over the Ohio Valley were depicted at 195 knots on the 300-hPa chart.

<sup>3</sup> Jet stream - A narrow band of strong wind in the atmosphere that controls the movement of high and low pressure systems and associated fronts. Jet Streams meander from time to time. Wind speeds can reach 200 mph or higher in certain cases. It is usually found at 30,000 to 40,000 feet above the earth's surface. It owes its existence to the large temperature contrast between the polar and equatorial regions. The position and orientation of jet streams vary from day to day. General weather patterns (hot/cold, wet/dry) are related closely to the position, strength and orientation of the jet stream (or jet streams).

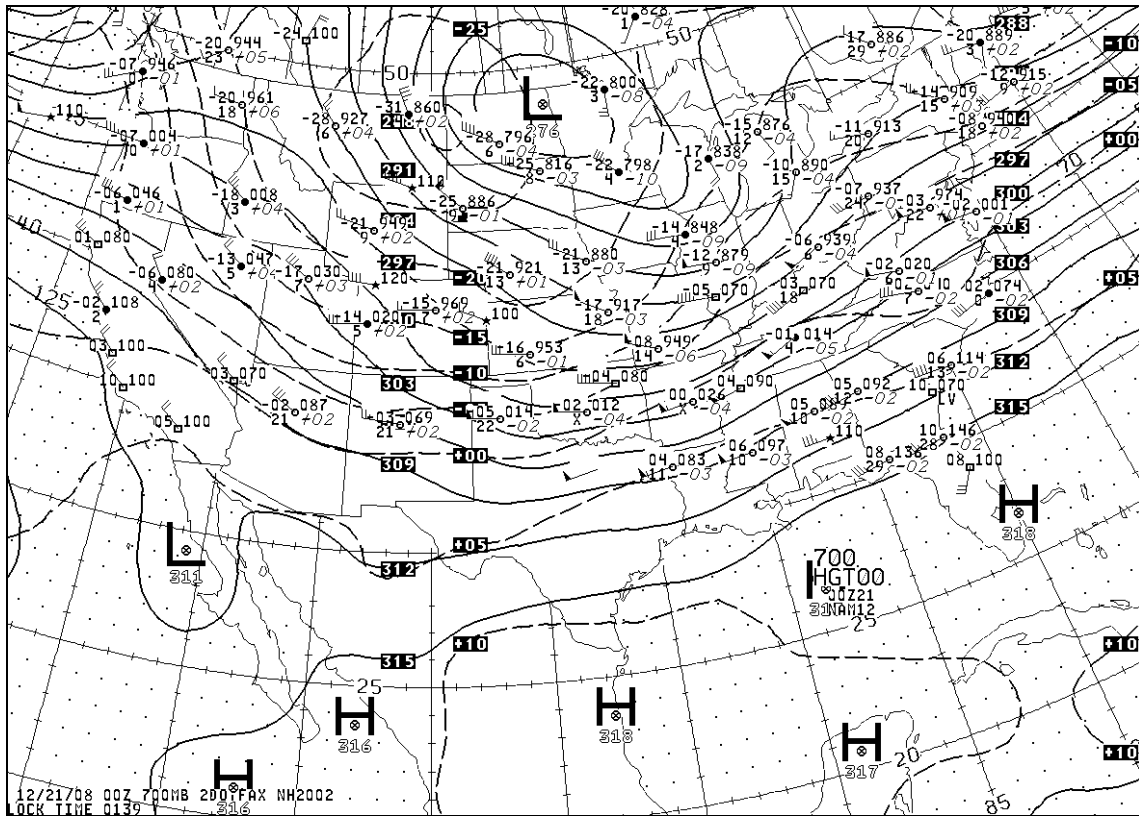


**Figure 3 – 700-hPa Constant Pressure Chart for 1700 MST**

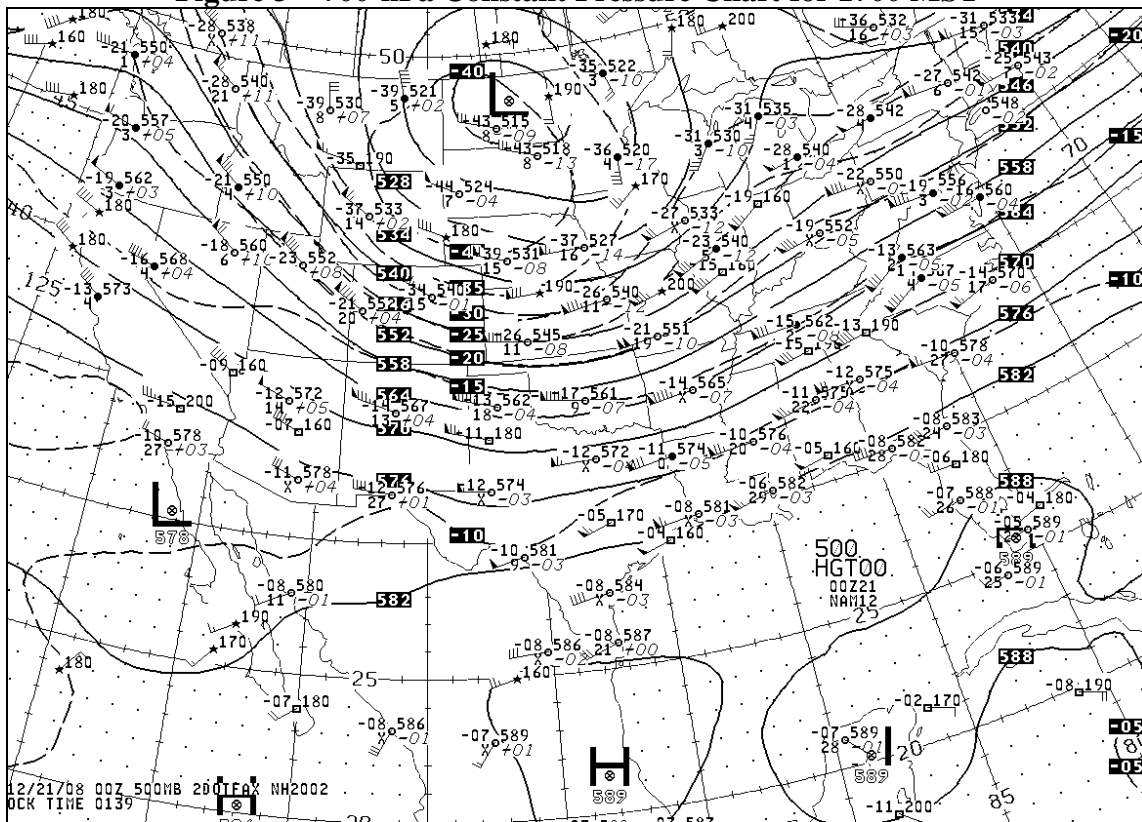




Figure 5 – 300-hPa Constant Pressure Chart for 1700 MST

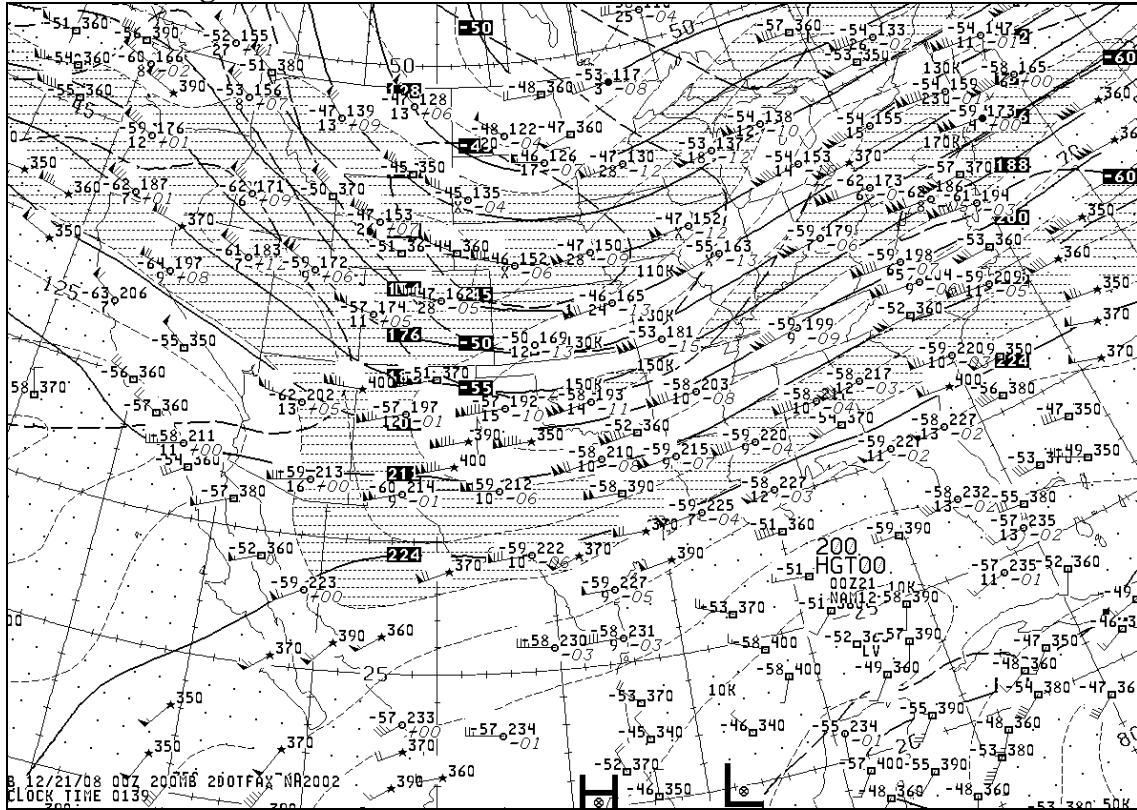


Figure 6 – 200-hPa Constant Pressure Chart for 1700 MST

### 1.0.3 Rapid Update Cycle (RUC) Models

Dr. Stanley Trier at NCAR provided further analysis of the synoptic and mesoscale meteorological conditions using the 13 km resolution Rapid Update Cycle (RUC) model (Benjamin et al. 2004). Dr. Tier indicated that the RUC model was particularly well-suited for this analysis, since it runs on an hourly cycle and assimilates numerous mesoscale observations, and including aircraft observations<sup>4</sup>.

The accident occurred approximately 36 hours after the passage of a large amplitude 500-hPa trough. The RUC model 500-hPa analysis from 1700 MST December 20, 2008 (0000Z on December 21, 2008) is included as figure 7 and indicated a strong 80 to 110 knot (40-55 m s<sup>-1</sup>) west to northwest flow over the Front Range of the Rocky Mountains upstream from the eastward progressing trough axis. Significant westerly flow is also evident closer to mountain top level at 700 hPa (figure 8), though its magnitude is 30 to 50 knots (15-25 m s<sup>-1</sup>) less than at 500-hPa, which indicated significant speed shear throughout a deep layer.

The earlier passage of the mid-level trough coincided with the southward movement of a shallow arctic air mass to the east the Rockies. In the corresponding RUC surface analysis this

<sup>4</sup> See section 3.0 of this report for an example of aircraft meteorological data through the ACARS Aircraft Meteorological Data Relay (AMDAR) system.

surface cold air mass, delineated by the blue colors (figure 9), has its western edge situated just east of KDEN (location indicated by cross) at 1700 MST.

West-to-East oriented vertical cross sections that intersect KDEN were constructed using RUC analyses in order to better depict the mesoscale ( $L > 50$  km) atmospheric structure in the vicinity of the accident. At 1700 MST (figure 10) the cross section shows westerly downslope flow, a local minimum of lower tropospheric relative humidity, and depressed midlevel potential temperature surfaces (figure 10B) consistent with mesoscale subsidence, extending approximately 100 km east of the mountains. This picture from the RUC analysis is supported by the lesser cloudiness observed in the satellite data (Section 4.0 of this report) and the deep dry adiabatic layer seen both in the Denver sounding and in the aircraft soundings in sections 2.0 and 3.0 of this report.

Embedded within the general westerly current is a quasi-stationary hydrostatic mountain wave (e.g., Klemp and Lilly 1978) with a westward tilting zone of enhanced flow in the immediate lee of the mountains indicated by the dashed gray line in figure 10. Downward motion associated with this wave may be contributing to the low relative humidity in this area. A second area of slightly enhanced westerly winds are evident extending downward to just a few hundred meters above the surface near KDEN and just west of the leading edge of the colder arctic air mass (figure 10(b)). A layer of higher stability above 4 km, was indicated by the packing of the potential temperature lines. This lies above a layer of nearly neutral stratification near and slightly above mountain top that extends for a significant distance upstream.

The vertical cross-section at 1800 MDT (0100Z) in figure 11, indicated the mountain wave feature persists. Enhanced westerly flow continued above KDEN, with slight reductions in relative humidity, which indicated continued subsidence flow. Figure 12 is the RUC analysis for 1900 MST (0200Z) which showed a slight expansion in the region of low relative humidity and enhancement of the vertical wind shear directly above KDEN.



RUC 500-hPa Winds, Height (solid), Temperature (dashed) and Relative Vorticity (colors)

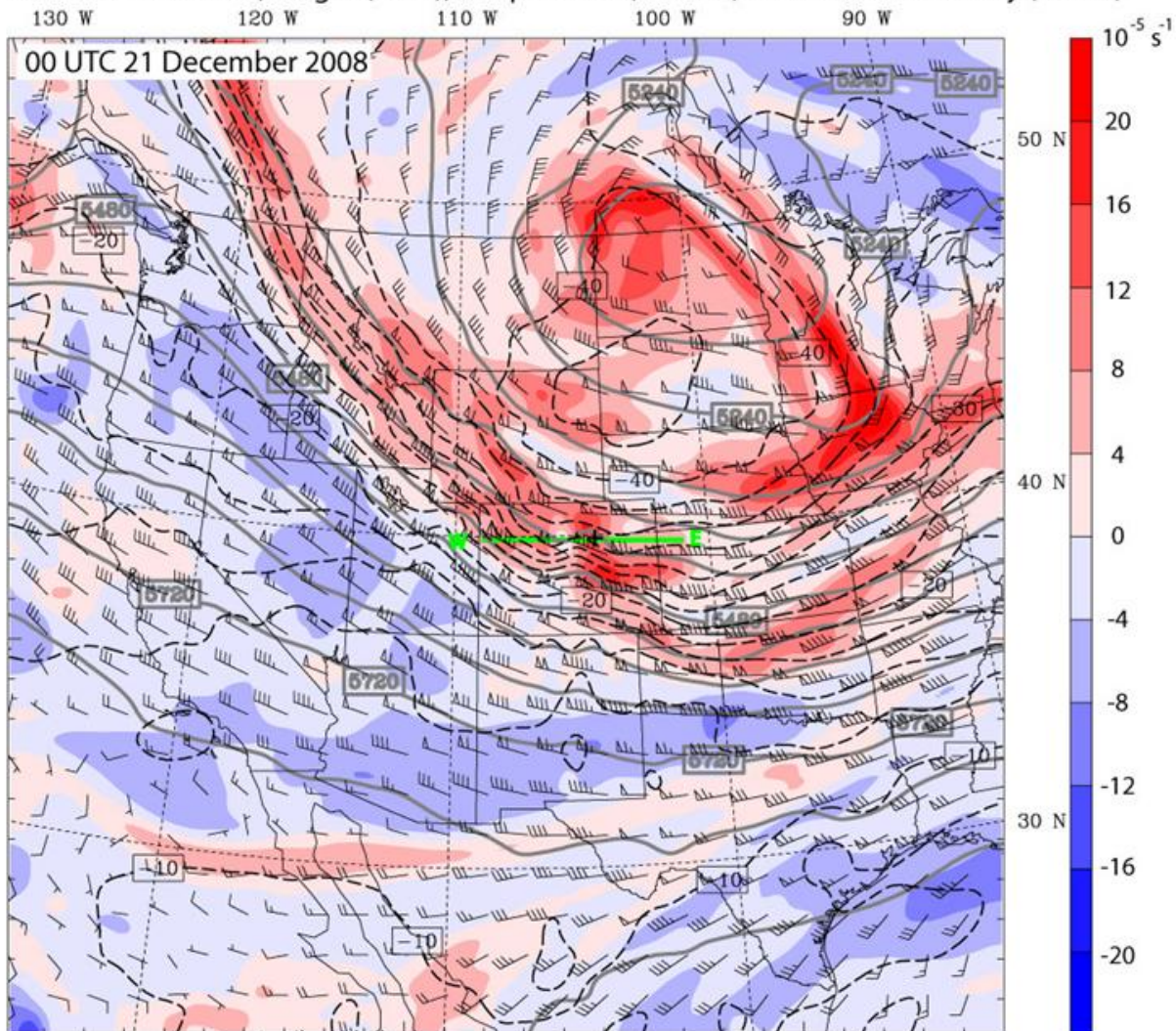


**Figure 7 - RUC 500-hPa Analysis (0-h forecast) for 1700 MST December 20, 2008. Horizontal winds have standard meteorological meaning with half barb =  $2.5 \text{ m s}^{-1}$  (5 kt), full barb =  $5 \text{ m s}^{-1}$  (10 kt)<sup>5</sup>, and pennant =  $25 \text{ m s}^{-1}$  (50 kt). Gray lines are the lines of geopotential heights at 60 meter contour intervals. The black dashed lines are lines of equal temperature or isotherms with  $2.5^\circ\text{C}$  contour interval, and colors are relative vorticity with the scale shown on the side. The green transect indicates the location of the vertical cross sections shown in figure 10. The “+” symbol indicates the location of KDEN.**

<sup>5</sup> kt – abbreviation for knots.

RUC 700-hPa Winds, Height (gray), Temperature (black) and Relative Humidity (colors)

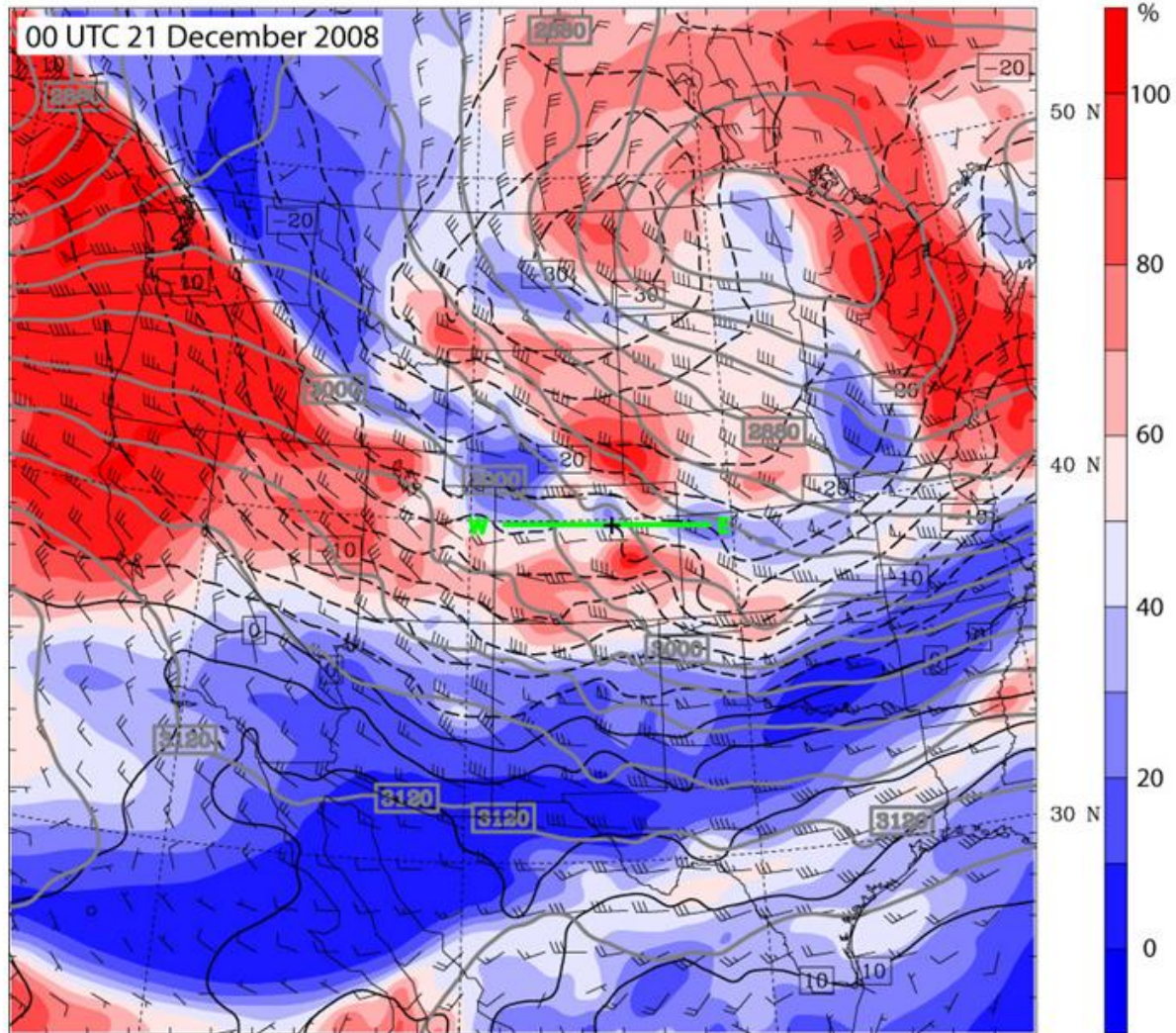


**Figure 8 – RUC 700-hPa Analysis for 1700 MST. Horizontal winds are as in figure 7. Gray lines are the geopotential heights with a 30 meter contour interval. Black lines are temperature with a 2.5° C contour interval, and the colored areas are relative humidity in percentage based on the color scale on the right.**

RUC Surface Winds, Sea-level Pressure (gray) and Surface Potential Temperature (colors)

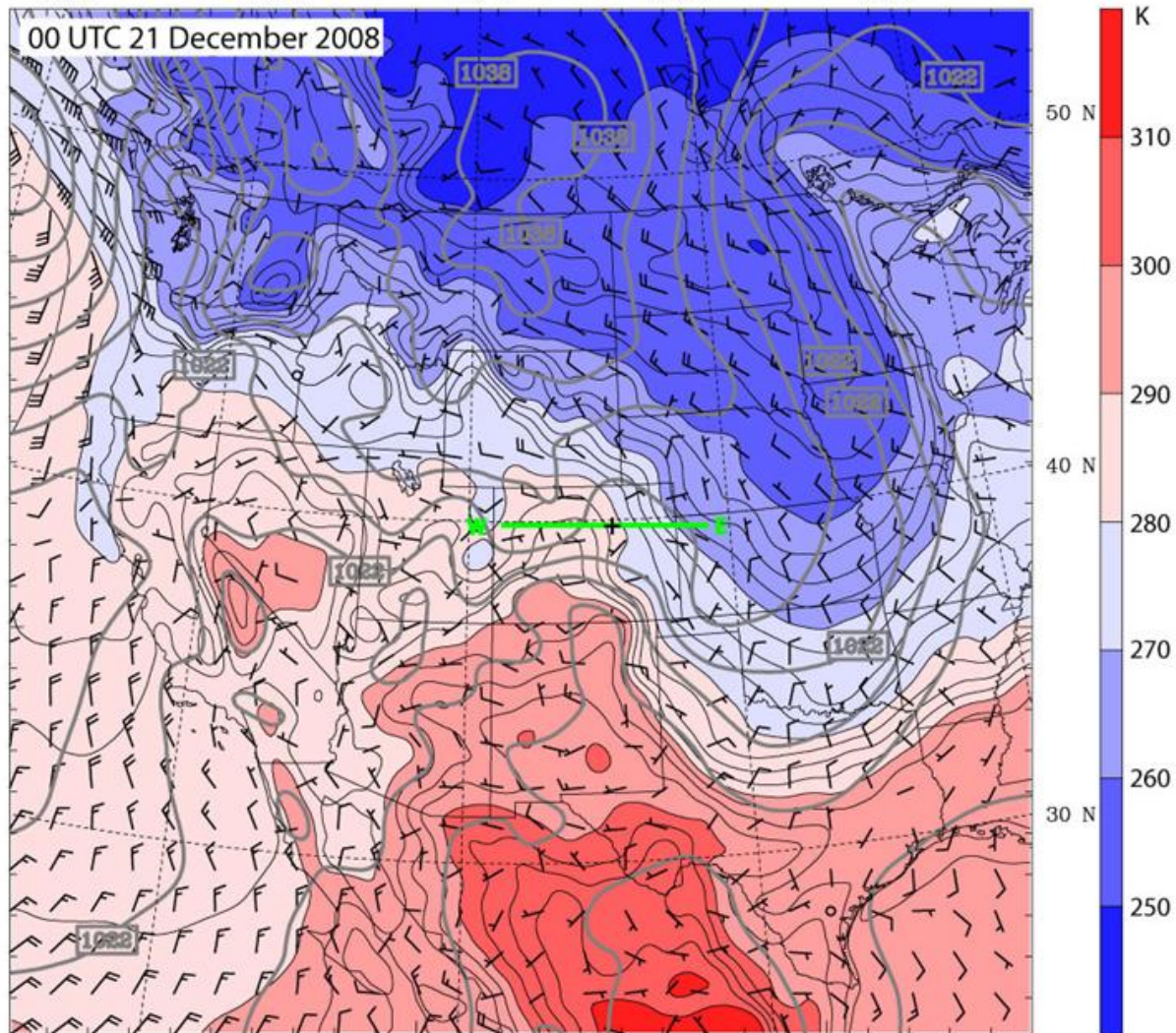
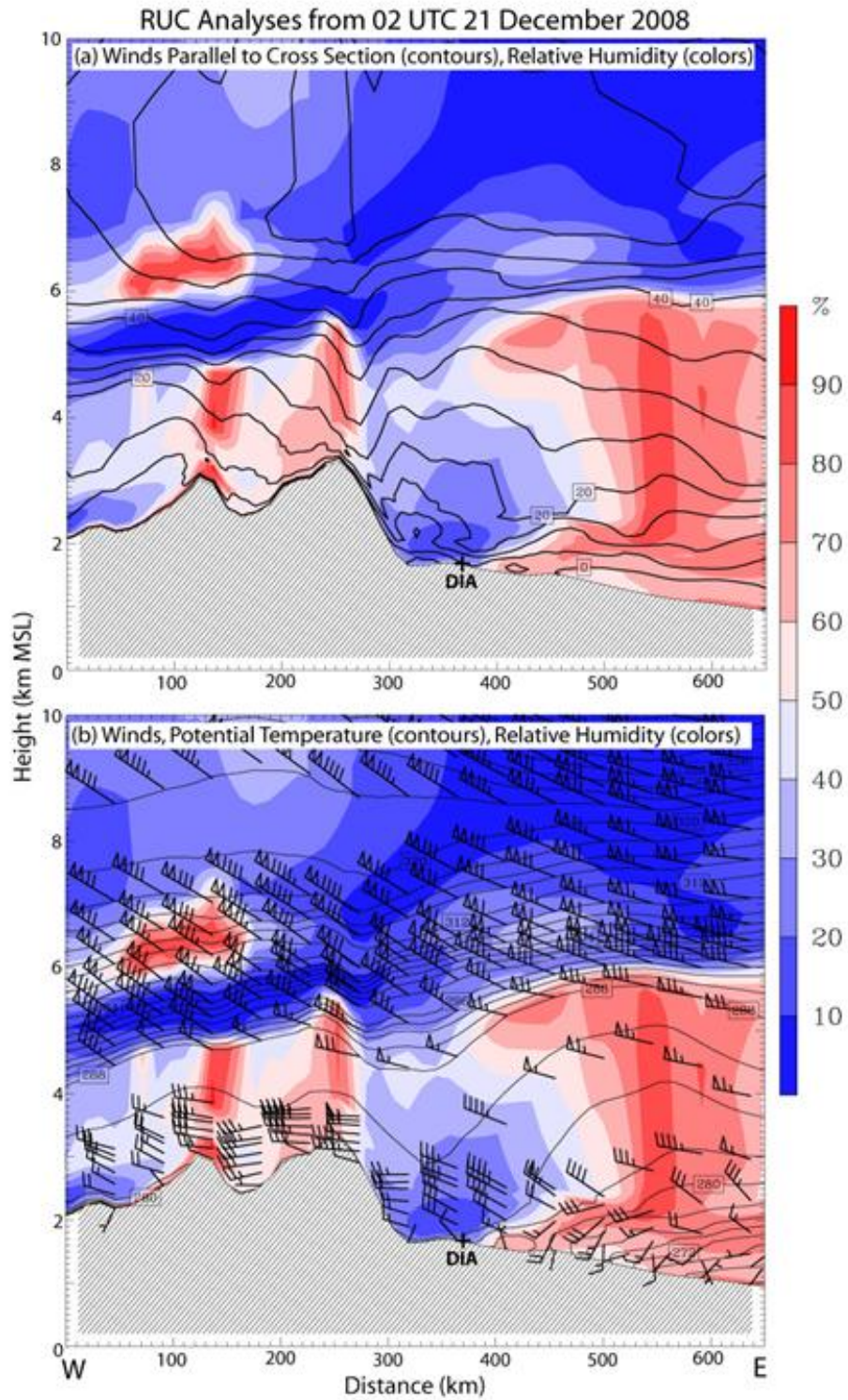


Figure 9 – RUC Surface Analysis for 1700 MST. Horizontal winds are as in figure 7. Gray lines are the geopotential heights with a 30 meter contour interval. Black lines are temperature with a 2.5° C contour interval, and the colored areas are relative humidity in percentage based on the color scale on the right.







**Figure 12 – 1900 MST (0200Z) RUC Analysis cross section**

Dr. Trier indicated that the RUC model plots show strong and persistent midlevel westerly/northwesterly flow combined with a stable layer above mountain top, favorable to the formation of mountain waves, present for the period surrounding the accident. However, several attributes of the large-scale environment differ from the “classic” conditions for mountain-wave induced strong downslope Boulder windstorms. For example, surface high pressure located to the north and east of the state of Colorado is not typical<sup>6</sup>. Also, the vertical shear through the troposphere is stronger than seen in the climatological study of Boulder windstorms<sup>7</sup>. In addition to the relatively strong vertical speed shear, another factor that could inhibit widespread strong downslope winds along the Front Range is the cold air mass just to the east of KDEN. The idealized numerical simulations of Lee et al. (1989)<sup>8</sup> illustrated the inability of strong westerlies to penetrate to the surface under these conditions and discussed how factors such as the depth of the cold air and the strength of the flow toward the mountains within the cold air were important predictors of whether strong downslope winds could eventually develop.

However, even though the environmental conditions may not have been ideal for a “classical” severe downslope windstorm (of the Boulder variety), other conditions were favorable for gusty surface winds near KDEN. First, the moderately strong flow over the mountains coupled with relatively weak large-scale surface flow promoted at least moderately strong low-level vertical shear evident near KDEN in the 1700 to 1900 MST (0000Z-0200Z) RUC analysis (figures 10 through 12). Second, the deep dry-adiabatic layer evident in Denver sounding approximately 1 hour prior to the accident (with the cold air mass still significantly to the east) suggests the potential for strong vertical mixing. Either vertical mixing or propagation effects associated with undulations in mountain waves for some distance downstream could explain localized regions of strong surface winds. The localization of strong surface winds presents potentially hazardous horizontal accelerations that are unresolved by both conventional observations and the RUC analyses, which have a relatively coarse horizontal grid spacing of approximately 13 kilometers (km) or 8 miles. Shorter wavelength lee waves, which could amplify in the stable layer, are also not resolved in the RUC analyses.

To determine the relation of the larger-scale pattern to the surface gusts observations at KDEN requires reconstruction of the event using high resolution computer simulations. In order to resolve partially trapped lee waves that may be present, and were observed in previous simulation studies of mountain wave wind events, the resolution must be much higher than the 13

---

<sup>6</sup> Mercer, A.E., M.B. Richman, H.B. Bluestein, and J.M. Brown, 2008: Statistical Modeling of Downslope Windstorms in Boulder, Colorado. *Weather and Forecasting*, 23, 1176–1194, and Neiman, P. J., R. M. Hardesty, M. A. Shapiro, and R. E. Cupp, 1988: Doppler lidar observations of a downslope windstorm. *Monthly Weather Review*, 116, 2265-2275.

<sup>7</sup> Brinkmann, W. A. R., 1974: Strong downslope winds at Boulder, Colorado. *Monthly Weather Review*, 102, 592–602.

<sup>8</sup> Lee, T. J., R. A. Pielke, R. C. Kessler, and J. Weaver, 1989: Influence of cold pools downstream of mountain barriers on downslope winds and flushing. *Monthly Weather Review*, 117, 2041-2058.

km used in the RUC model. Thus a multi-nested nonhydrostatic simulation model with the finest horizontal resolution of 250 meters (m) over the KDEN area was setup and executed to better duplicate the atmospheric structures at the time of the event. These model results are presented and discussed in section 7.

## 2.0 Upper Air Sounding

The Denver upper air sounding or rawinsonde observation (RAOB) was obtained from the NWS Denver (KDNR), Colorado, site number 72469, at an elevation of 5,331 feet msl. The 1700 MST (0000Z sounding on December 21, 2009) from KDNR plotted on a standard Skew-T log P diagram<sup>9</sup> with the observed and derived stability parameters and is included as figure 13 from the surface to 200-mb or 39,000 feet.

The KDNR entire sounding was below freezing. The sounding depicted a dry low-level environment with the lifted condensation level (LCL)<sup>10</sup> at 668-hPa or 5,596 feet agl (10,927 feet msl), a convective condensation level (CCL)<sup>11</sup> at 630-hPa or at 7,035 feet agl (12,366 feet msl), and a level of free convection (LFC)<sup>12</sup> at 597-hPa or 8,298 feet agl (13,629 feet msl). The sounding depicted a dry environment except between 12,000 and 15,000 feet where the relative humidity was near 70 percent. The precipitable water value was 0.10 inches. The sounding depicted a defined temperature inversion due to subsidence between 17,000 and 20,000 feet. The tropopause height was identified at 33,454 feet.

---

<sup>9</sup> Skew T log P diagram – is a standard meteorological plot using temperature and the logarithmic of pressure as coordinates, used to display winds, temperature, dew point, and various indices used to define the vertical structure of the atmosphere.

<sup>10</sup> Lifting Condensation Level (LCL) - The height at which a parcel of moist air becomes saturated when it is lifted dry adiabatically.

<sup>11</sup> Convective Condensation Level (CCL) - The height to which a parcel of air, if heated sufficiently from below, will rise adiabatically until condensation starts. This is typically used to identify the base of cumuliform clouds, which are normally produced from surface heating and thermal convection.

<sup>12</sup> Level of Free Convection (LFC) -The level at which a parcel of saturated air becomes warmer than the surrounding air and begins to rise freely. This occurs most readily in a conditionally unstable atmosphere.



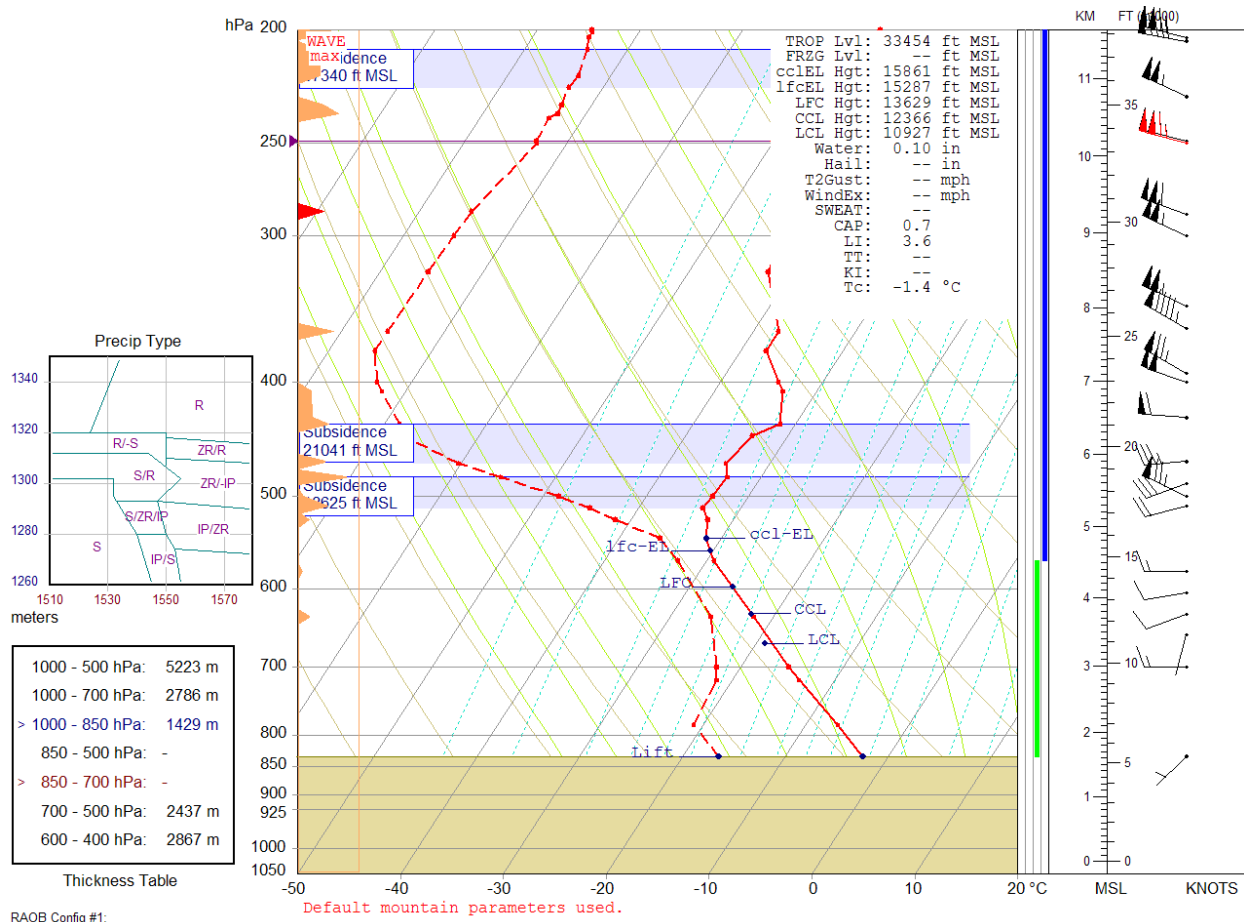


**Figure 13 –KDNR 1700 MST (0000Z) sounding**

The sounding wind profile on the right indicated surface winds from 225° at 3 knots with winds veering to the west immediately above the surface and then to the west-northwest increase in speed with height, with the maximum wind in the immediate vicinity of the tropopause at 33,368 feet from 285° at 115 knots.

The left side of sounding depicts the RAOB’s analysis program for mountain wave activity (shown in orange). The sounding depicted multiple waves over the Denver area at the time, and were further supported by the thermal and wind fields.

Table 1 is the observed height, pressure, temperature, dew point, relative humidity (RH), wind direction and speed, and RAOB analysis information on clear air turbulence (CAT) and mountain wave activity.

Level	Height (ft-MSL)	Pres (hPa)	T (C)	Td (C)	RH (%)	DD / FF (deg / kts)	CAT (FAA)	LLWS	Icing - Type (AF @ 75% RH)	Wave/X--W--Turb nm fpm max
1	5331	834.0	-2.5	-16.5	33	225 / 3				
2	6927	784.0	-6.9	-20.9	32					
3	9151	718.0	-13.5	-21.5	51					
4	9783	700.0	-15.3	-22.3	55	270 / 15	MDT			
5	11331	657.1				195 / 1				
6	12207	634.0	-21.9	-26.1	69		SVR		2.21	305 LIGHT
7	12331	630.7				250 / 12				
8	13331	604.8				260 / 11	LGT			
9	14331	579.9				270 / 16			7.47	182 LIGHT
10	14823	568.0	-29.3	-32.8	72					
11	15873	543.0	-31.5	-36.0	64					
12	16699	524.0	-32.5	-41.5	40				2.91	344 LIGHT
13	17234	512.0	-33.7	-44.7	32					
14	17331	509.8				255 / 22	XTR		2.39	708 LT-MD
15	17780	500.0	-33.5	-48.5	21	295 / 73	XTR		4.30	188 LIGHT
16	18331	488.2				250 / 31				
17	18625	482.0	-33.3	-55.3	9				3.81	1960 SEVERE
18	19254	469.0	-34.3	-60.3	5		MDT			
19	19331	467.4				265 / 33			3.37	751 LT-MD
20	20514	444.0	-33.5	-67.5	2					
21	21041	434.0	-31.5	-68.5	1		SVR		3.62	856 LT-MD
22	21331	428.6				275 / 59			6.33	574 LIGHT
23	22527	407.0	-33.3	-72.3	1		XTR		14.54	666 LIGHT
24	22926	400.0	-34.3	-73.3	1	290 / 101	XTR			
25	23331	393.0				300 / 77				
26	24337	376.0	-37.5	-75.5	1					
27	25196	362.0	-37.5	-75.5	1		MDT		9.67	1541 MD-SV
28	25331	359.8				300 / 96	SVR			
29	26331	344.1				295 / 103				
30	27821	322.0	-42.3	-75.3	2					
31	29388	300.0	-43.1	-75.1	2	295 / 104	SVR			
32	30331	287.5				290 / 109				
33	30443	286.0	-43.9	-74.9	2		LGT		15.50	1177 LT-MD
34	33368	250.0	-49.9	-72.9	5	285 / 115				
35	33454	249.0	-50.1	-73.1	5	285 / 115				
36	34422	238.0	-50.3	-73.3	5					
37	34603	236.0	-48.7	-72.7	5				6.35	1701 MD-SV
38	34972	232.0	-47.9	-72.9	4		SVR		8.03	991 LT-MD
39	35331	228.2				295 / 105				
40	35731	224.0	-48.3	-73.3	4					
41	36220	219.0	-47.1	-73.1	4				6.72	804 LT-MD
42	37340	208.0	-46.9	-73.9	3				9.21	868 LT-MD
43	37868	203.0	-47.5	-74.5	3					
44	38083	201.0	-46.5	-74.5	3		SVR		7.55	2020 MD-SV
45	38192	200.0	-46.7	-74.7	3	280 / 91	XTR			
46	38331	198.7				285 / 115				
47	39196	191.0	-45.9	-74.9	2				7.33	619 LIGHT
48	40128	183.0	-46.9	-74.9	3				10.97	687 LIGHT
49	41873	168.0	-50.5	-74.5	4					

**Table 1 – KDNR observed and derived sounding parameters**

### 3.0 Aircraft Derived Soundings

The NOAA Forecast System Laboratory (FSL) Aircraft Meteorological Data Relay (AMDAR) was also reviewed and aircraft soundings immediately surrounding the accident were documented. There were two aircraft reports made within 15-minutes surrounding the accident; aircraft #302 at 1802 MST and. Aircraft #770 at 1827 MST. The ascent/descent reports from these aircraft follows.

Aircraft identified as #302, departed at 1802 MST (0102Z) from KDEN with a destination of Norman Y. Mineta San Jose International Airport (KSJC). Figure 14 is the aircraft's ascent sounding, followed by a table of observed data. The aircraft departed to the west (runway 25) and reported at 6,010 feet a wind from 280° at 34 knots, and a temperature of -5.0° C. The wind profile showed winds increase with height and veering slightly to the west-northwest with height, with a maximum wind of 158 knots at 28,000 feet. The sounding also confirmed an inversion or stable layer between 16,000 and 24,000 feet.

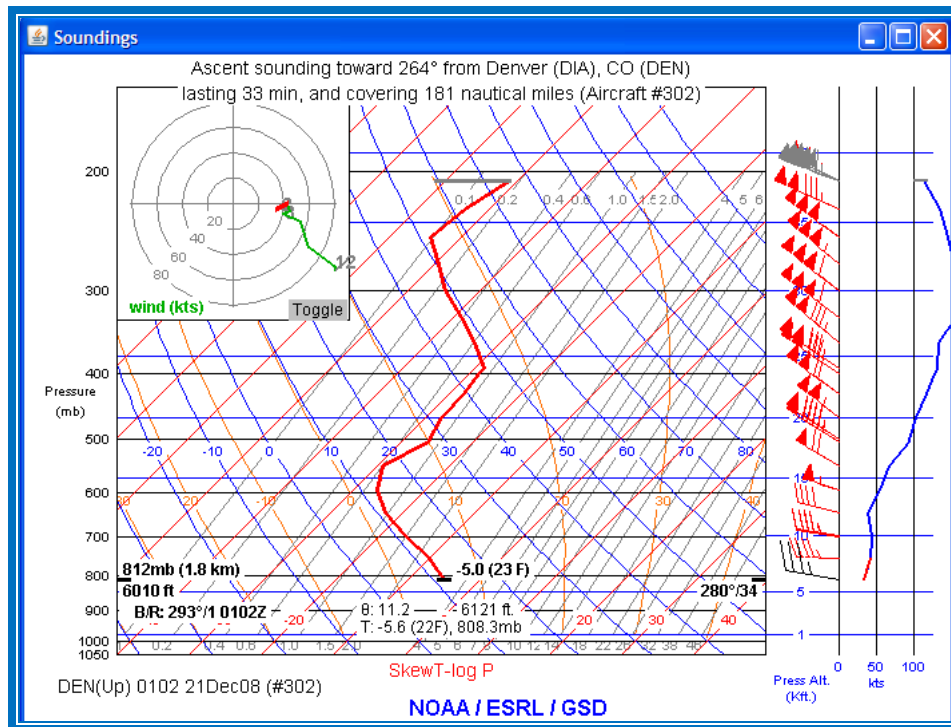


**Figure 14 – AMDAR aircraft sounding at 1802 MDT**

P_alt (ft)	mb	t/td (°C)	w_dir/w_spd (kts)	Time (UTC)	Bng/Rng (nm)
6010	812	-5.0/-----	280°/034	0102	293°/001
8020	752	-10.0/-----	271°/043	0103	304°/003
9882	700	-16.1/-----	279°/046		
10000	697	-16.5/-----	279°/046	0104	298°/008
12050	643	-22.5/-----	283°/040	0105	288°/012
14010	595	-26.8/-----	286°/056	0106	283°/014
16030	548	-29.3/-----	300°/069	0107	280°/017
18000	506	-26.3/-----	302°/095	0107	278°/020
18287	500	-26.5/-----	303°/096		
20020	465	-27.8/-----	307°/104	0108	275°/023
22030	427	-28.0/-----	305°/118	0108	274°/026
23571	400	-28.6/-----	303°/130		
24040	392	-28.8/-----	303°/133	0109	273°/030
26000	360	-33.5/-----	310°/134	0110	271°/035
28000	329	-39.0/-----	306°/158	0112	270°/044
30020	301	-44.8/-----	307°/158	0113	269°/051
30065	300	-44.9/-----	307°/158		
32000	274	-49.5/-----	309°/156	0114	268°/057

Figure 15 is the descent sounding from an aircraft identified as #770, arriving from Sacramento International Airport (KSMF) at 1827 MST (0127Z). At 6,000 feet, the aircraft reported a wind from 277° at 39 knots and a temperature of -5.3° C. The wind profile also showed little variation in direction with height with winds veering to the west-northwest with height, with the maximum wind from 292° at 113 knots at 28,000 feet. An inversion was also noted between 18,000 and 24,000 feet.

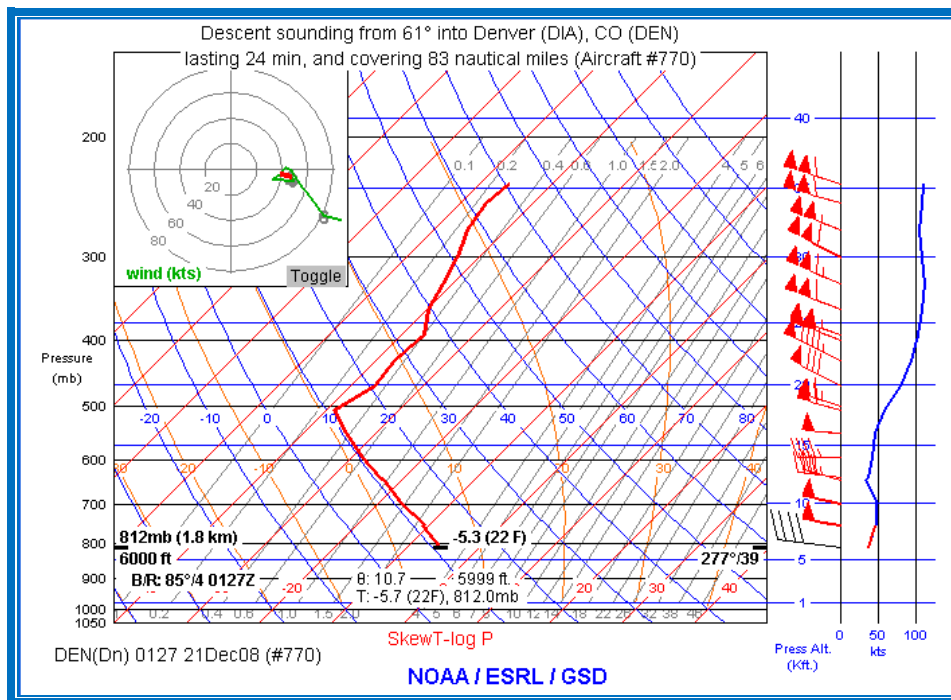


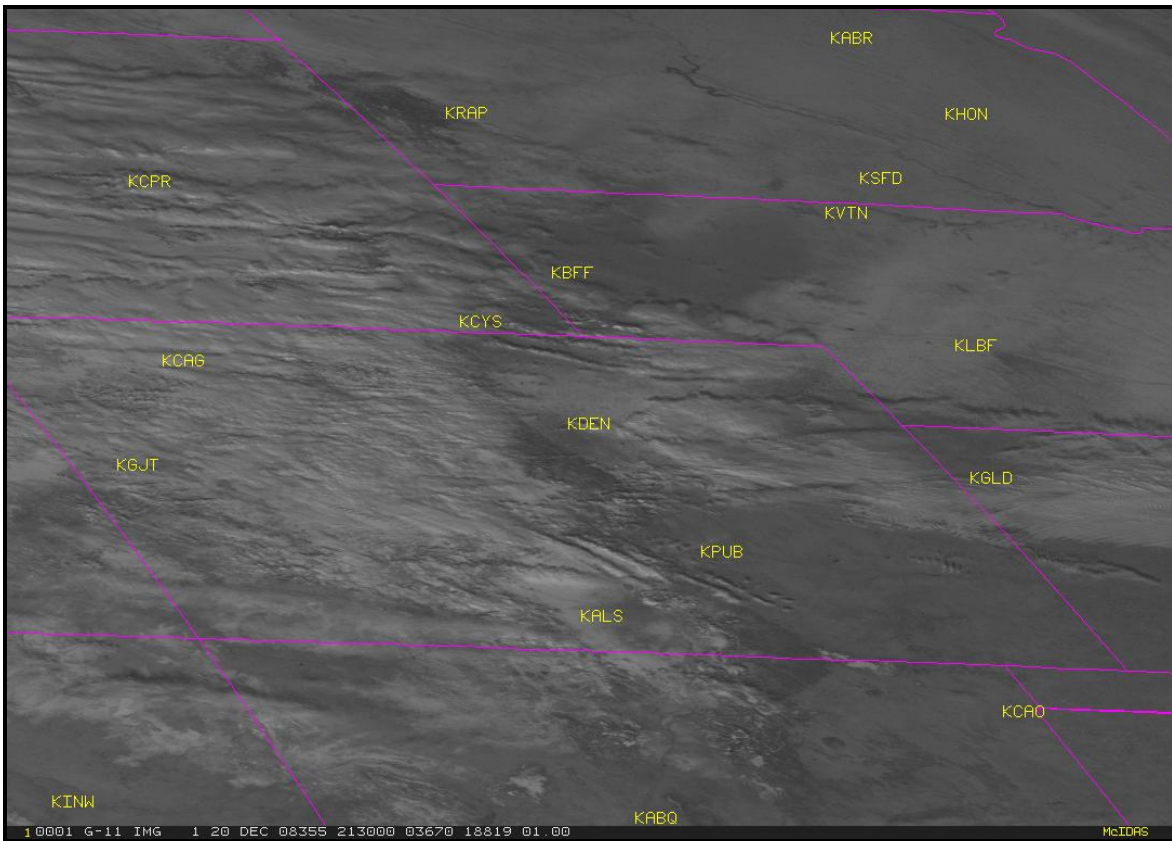
Figure 15 – AMDAR descent sounding at 1827 MST

P_alt (ft)	mb	t/td (°C)	w_dir/w_spd (kts)	Time (UTC)	Bng/Rng (nm)
6000	812	-5.3/-----	277°/039	0127	85°/004
8000	753	-10.8/-----	278°/048	0123	88°/010
8120	749	-10.8/-----	278°/049	0123	89°/011
9882	700	-16.4/-----	281°/050		
10000	697	-16.8/-----	281°/050	0119	88°/019
12000	644	-22.3/-----	285°/034	0117	78°/023
12240	638	-23.3/-----	277°/039	0117	75°/024
13990	595	-28.5/-----	269°/043	0113	46°/034
15980	550	-34.0/-----	273°/048	0111	46°/042
17960	507	-39.0/-----	285°/059	0109	51°/050
18287	500	-38.6/-----	287°/063		
19960	466	-36.8/-----	297°/082	0108	53°/054
22000	428	-37.5/-----	295°/095	0107	54°/058
23572	400	-36.9/-----	289°/102		
24000	393	-36.8/-----	288°/104	0107	56°/062
25990	360	-39.8/-----	290°/110	0106	57°/066
27990	329	-41.3/-----	292°/113	0105	58°/070
29940	302	-43.0/-----	297°/110	0105	59°/073
30064	300	-43.1/-----	297°/110		

#### 4.0 Satellite Imagery

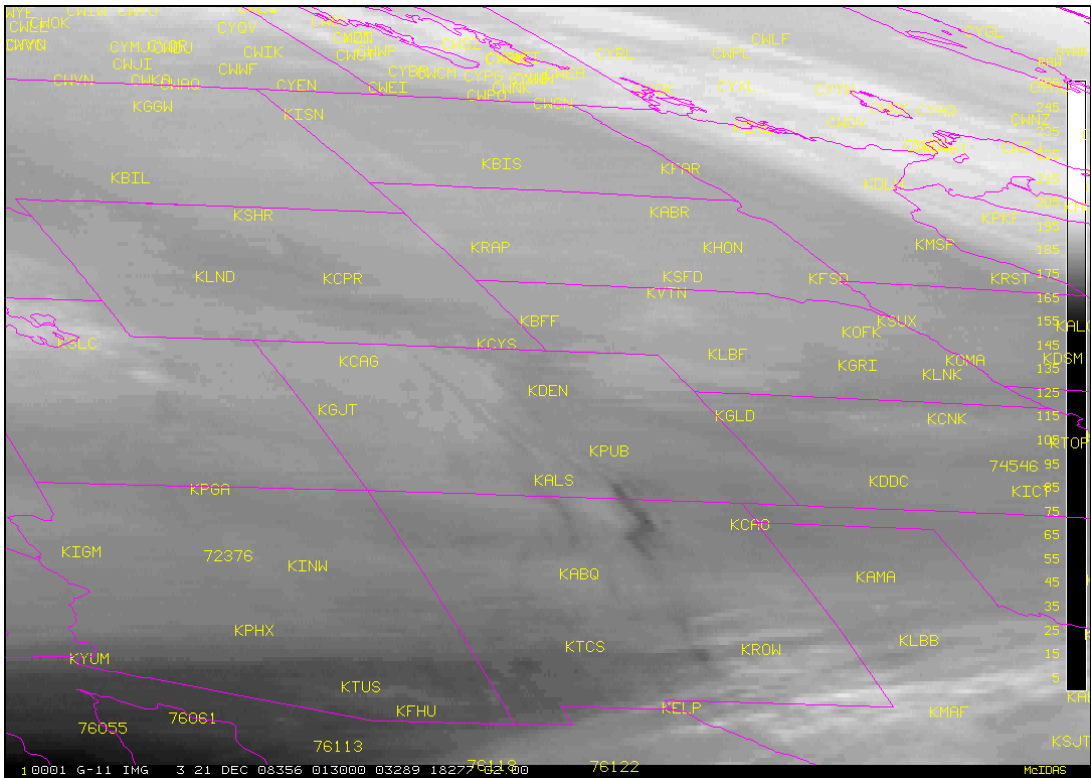
The Geostationary Operations Environmental Satellite number 11 (GOES-11) data was obtained from the National Climatic Data Center (NCDC) and displayed on the National Transportation Safety Board’s Man-computer Interactive Data Access System (McIDAS) workstation. Both visible, water vapor, and infrared imagery were obtained surrounding the time of the accident. The infrared imagery (band 4) at a wavelength of 10.7 microns ( $\mu\text{m}$ ) provided a 4-kilometer (km) resolution with radiative cloud top temperatures. The water vapor or moisture channel (band 3) at a wavelength of 6.5 to 7.0  $\mu\text{m}$  provided an 8-km resolution, and the visible imagery (band 1) at a wavelength of 0.65  $\mu\text{m}$  provided a resolution of 1 km. The satellite imagery surrounding the time of the accident from 1300 through 2000 MST (2000Z through 0200Z), at approximately every 15-minutes were reviewed and the closest images documented below.

Figure 16 is the GOES-11 visible (band 1) image at 1430 MST (2130Z). The image depicted KDEN in a clear zone with a band of low to mid-altitude clouds east, and an extensive area to the west over the mountains. A north to south oriented clear notch runs parallel to the Rockies (darker zone), that extends from west of Cheyenne Airport, Wyoming (KCYS), Denver International Airport (KDEN) and Pueblo Memorial Airport, Colorado (KPUB).



**Figure 16 – GOES-11 visible image at 1430 MST**

Figure 17 and 18 are the GOES-11 water vapor and infrared images at 1830Z (0130Z) at 2X magnification respectively. A north-to-south band of moisture channel darkening is observed west of KDEN and is also indicated slightly in the infrared image, suggesting downward motion or warming to the lee of the Rockies, a characteristic often noted in mountain wave and downslope wind conditions. Cap clouds and lenticular clouds are also observed in the vicinity, which do not move with the mean winds and remain stationary with time, while clouds downstream or east of Denver show signs of strong low-level westerly winds.



**Figure 17 – GOES-11 water vapor image at 1830 MST**

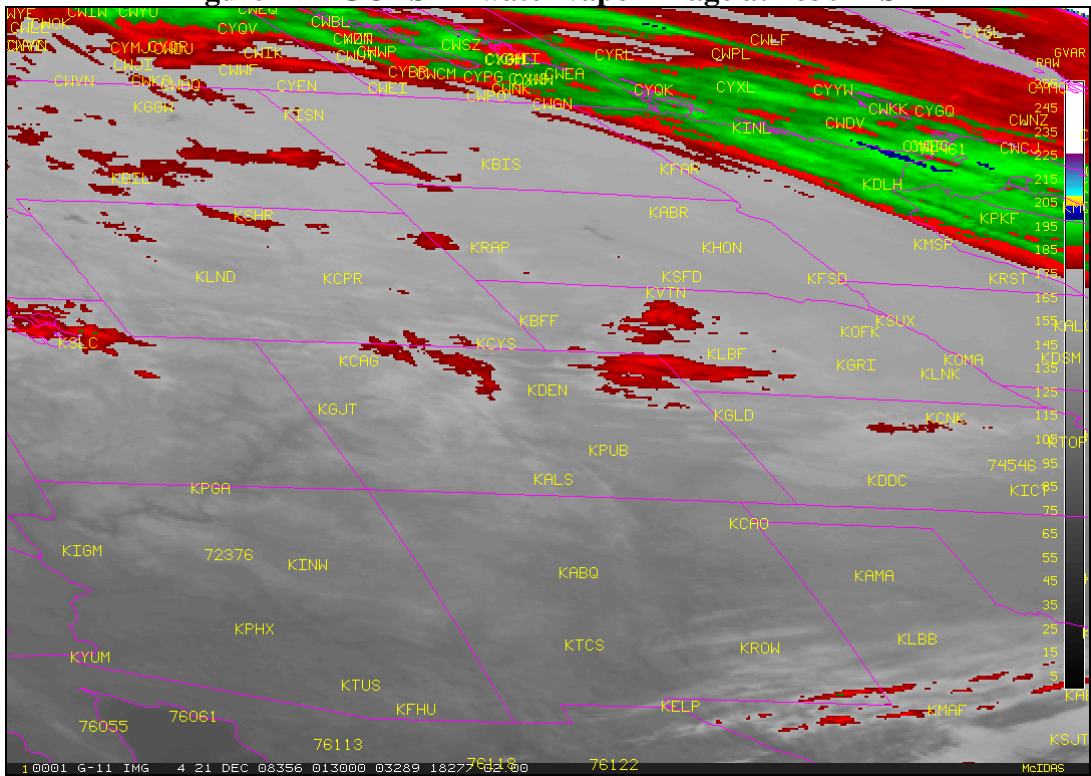


**Figure 18 – GOES-11 infrared image at 1830 MST**

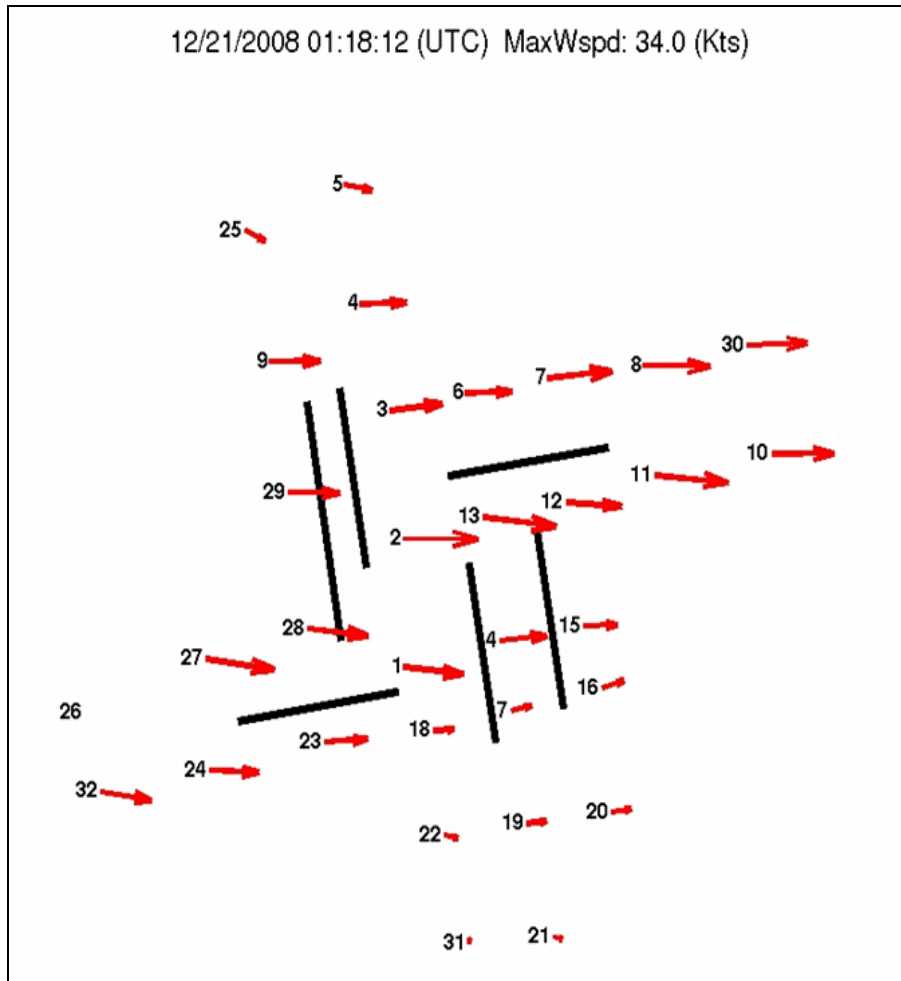
## 5.0 NCAR LLWAS Review

Dr. Larry B. Cornman of the National Center of Atmospheric Research (NCAR) provided a detailed briefing of his Low Level Windshear Alert System (LLWAS)<sup>13</sup> wind analysis to the NTSB on September 9, 2009. He plotted the KDEN LLWAS-NE wind vectors and showed an animation from 1813 to 1823 MST (0113Z to 0116Z), which depicted a band of strong westerly winds centered over Denver International Airport during the period, with the maximum 10-second LLWAS wind of 40 knots reported approximately 2-minutes prior to the accident from sensor number 2. Of particular interest in the animation, immediately north and south of the airport, lighter wind was noted by the LLWAS system and a pulsing pattern was observed with wind speeds increasing, decreasing, and then increasing again. Figure 19 is the 1818:12 MST (0118:12Z) LLWAS wind plot at the approximate time of the accident, with the sensor numbers indicated in black. The maximum 10-second average wind speed of all the sensors at the time of the accident was 34 knots, which was reported at sensor number 2. Dr. Cornman emphasized that the LLWAS wind sampling does not account for wind gusts, and thus the actual wind speeds due to peak gusts were likely higher than what was depicted. Attachment 6 is the NCAR presentation on the LLWAS and wind vectors at 1818:12 MST.

---

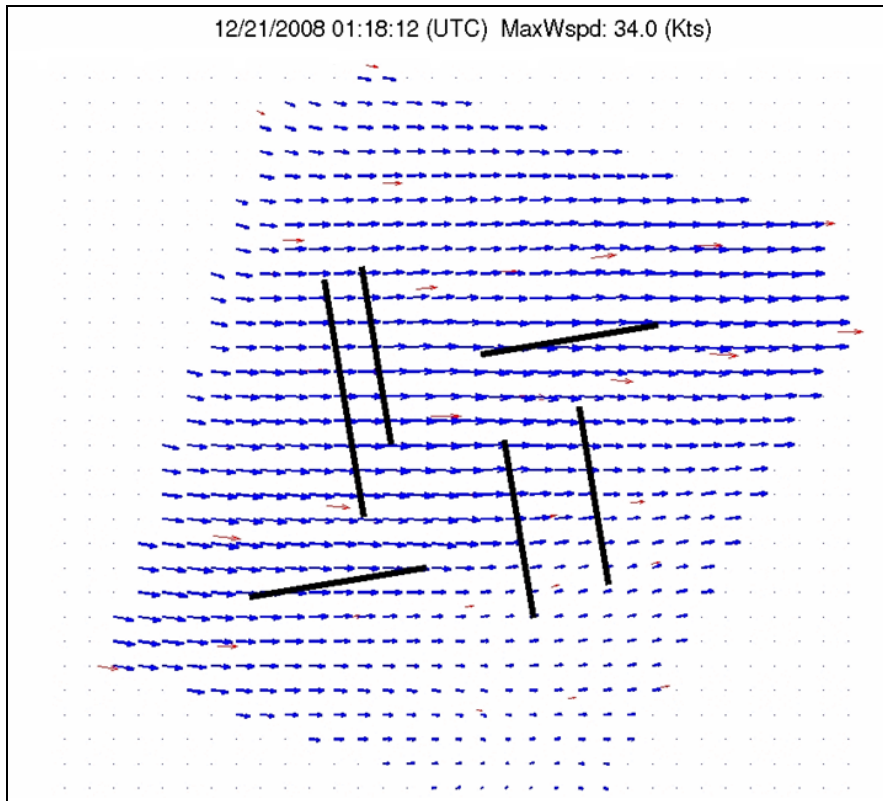
<sup>13</sup> The Denver system is actually a LLWAS-NE++ system or Low-Level Windshear Alert System - Network Expansion Rehost, with 32 sensors, with winds reported in degrees magnetic for Air Traffic Control and runway oriented wind use.





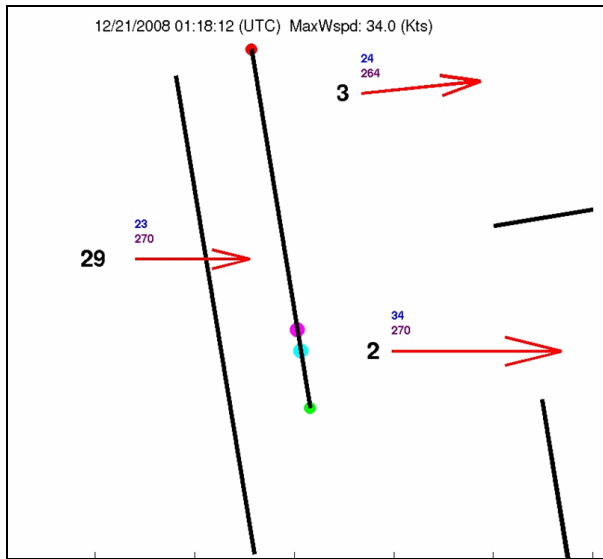
**Figure 19 – LLWAS wind field at 1818 MST**

Figure 20 is an interpolation of the wind field between stations, with the LLWAS data shown in red. The image depicts the band of high winds concentrated over the center of the airport with lighter winds indicated north and south of the center of the airport, with a potential wind reversal to the south.



**Figure 20 – Interpolated wind field at 1818 MST**

An animation was also created based on LLWAS sensors number 29, 2, and 3 immediately surrounding runway 34R and the accident site. Figure 21 is the plot of the wind at the time of the accident and indicates LLWAS 10-second winds from  $264^{\circ}$  to  $270^{\circ}$  at 23 to 34 knots. LLWAS sensor number 2 was the closest wind sensor to the location where the aircraft left the runway 34R, and also had the highest reported wind of 34 knots at the time. As reported in the Air Traffic Control Factual Report, the tower provided wind information from sensor number 3 as the departure wind for runway 34R.



**Figure 21 – LLWAS sensors surrounding the accident site**

Figure 22 is a plot of the LLWAS crosswind component for departure of runway 34R from sensors 2 and 29.

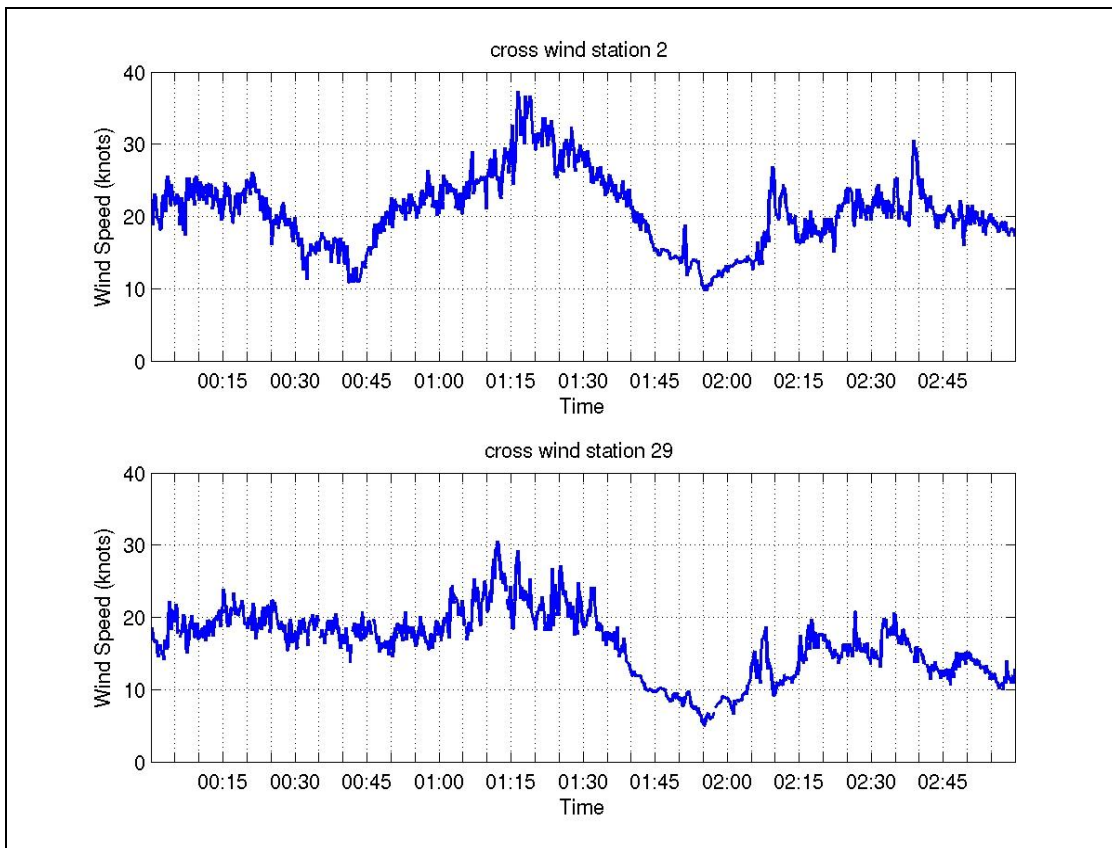


**Figure 22 – Crosswind factor for runway 34R departure based on sensors 2 and 29**

## 6.0 Mountain Wave Conditions

As indicated in other sections of this report, conditions were favorable for mountain wave activity over the Rocky Mountains on the day of the accident. In addition, there was evidence of waves in the satellite imagery (see section 4.0). In fact, mountain waves and mountain wave turbulence were reported by pilots in the area throughout the day (see section 8.0).

A fundamental question is whether or not the gustiness reported at KDEN could be related to mountain wave activity. In this section a brief review of mountain wave concepts is provided, which are helpful in understanding the results of the numerical model simulations that follow in section 7.0.

### 6.0.1 Background

Air flowing over mountainous terrain often generates atmospheric gravity waves (so named because gravity is the restoring force), also called “mountain waves”. Mountain wave patterns produced by air flow over the same mountain range can differ dramatically depending on the vertical variation of wind and temperature in the upstream atmospheric flow as in figure 23 (from Durran and Klemp 1983, [www.comet.ucar.edu](http://www.comet.ucar.edu)). The left image in figure 23 illustrates a long wavelength, vertically propagating mountain waves in which the wave motion is primarily located above the mountain crest. This would typically occur in an atmospheric profile with no vertical variation of wind or stability with height. Under extreme conditions these waves may have features analogous to “hydraulic jumps”. In contrast, under other atmospheric conditions waves may be vertically trapped, propagating horizontally far downstream, referred to as “lee waves”, which is depicted on the right of figure 23. This typically occurs when wind increase rapidly with height, or rapidly decreasing stability. Both vertically and horizontally propagating waves can create lee side accelerations. Realistic atmospheric profiles often result in a combination of vertically propagating waves and partially trapped lee waves<sup>14</sup>.

---

<sup>14</sup> Multiple authors include: Wurtele, M. G., R. D. Sharman, and T. L. Keller, 1987. Analysis and simulations of a troposphere-stratosphere gravity wave model, Part I. *Journal of Atmospheric Science*, 44, 3269-3281, Sharman, R. D., and M. G. Wurtele, 2004: Three-dimensional structure of forced gravity waves and lee waves. *Journal of Atmospheric Science*, 61, 664-680, and Keller, T. L. 1994. Implications of the hydrostatic assumption on atmospheric gravity waves. *Journal of Atmospheric Science*, 51, 1915-1929.

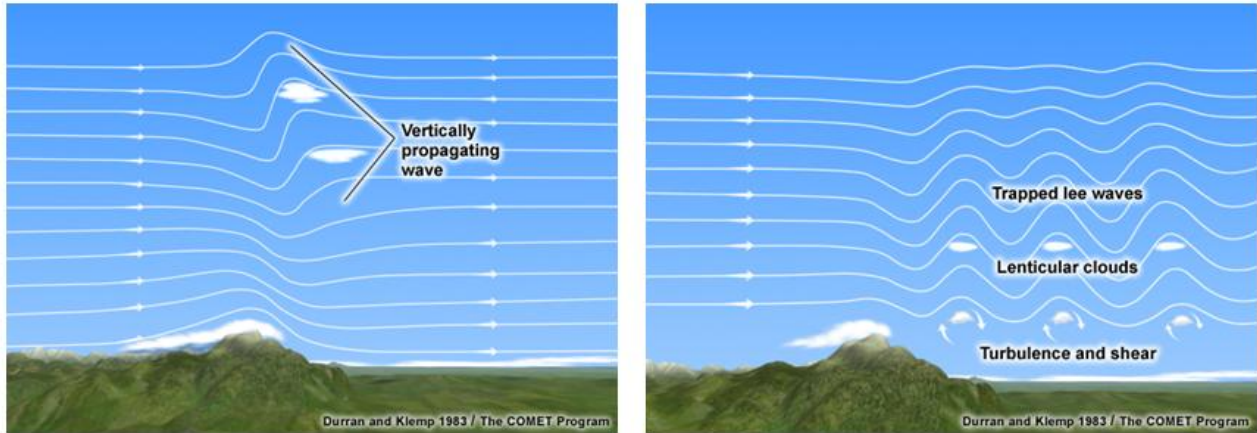


**Figure 23 – Mountain waves under different atmospheric conditions. (a) vertical propagating waves (b) horizontal propagating trapped “lee waves”.**

Of particular importance to this case, it is well-known that large amplitude lee waves can induce significant wind and pressure perturbations at the surface, sometimes resulting in regions of reversed flow and low-level rotor structures<sup>15</sup>. Note that lee waves are known to amplify in a stable layer near mountain top<sup>16</sup>, as was observed during the time of the KDEN accident. Capturing the effects of an elevated stable layer, represented by an inversion layer atop a deep neutral layer, Vosper (2004) found the inversion height, relative to the mountain height, was important in determining the transition from a regime with large amplitude lee waves to a regime with hydraulic jump like flow, such as occurs with severe downslope windstorms.

Mountain waves may also break aloft causing turbulence such as often encountered by aircraft over the Rocky Mountains west of Denver. Figure 24 illustrates a breaking mountain wave, hydraulic jump like behavior, and downslope windstorms<sup>17</sup>. This is also documented the Federal Aviation Administration (FAA) Advisory Circular 00-57 “Hazardous Mountain Winds and their Visual Indicators”.

<sup>15</sup> Doyle, J.D., and D.R. Durran, 2002: The Dynamics of Mountain-Wave-Induced Rotors. *Journal of Atmospheric Science*, 59, 186–201, and Vosper, S. B., 2004: Inversion effects on mountain lee waves. *Quarterly Journal of the Royal Meteorology Society*, 130, 1723–1748.

<sup>16</sup> Ralph, F.M., P.J. Neiman, T.L. Keller, D. Levinson, and L. Fedor, 1997: Observations, Simulations, and Analysis of Nonstationary Trapped Lee Waves. *Journal of Atmospheric Science*, 54, 1308–1333.

<sup>17</sup> Whiteman, C. D., 2000: *Mountain Meteorology: Fundamentals and applications*. Oxford University Press, 355 pp.

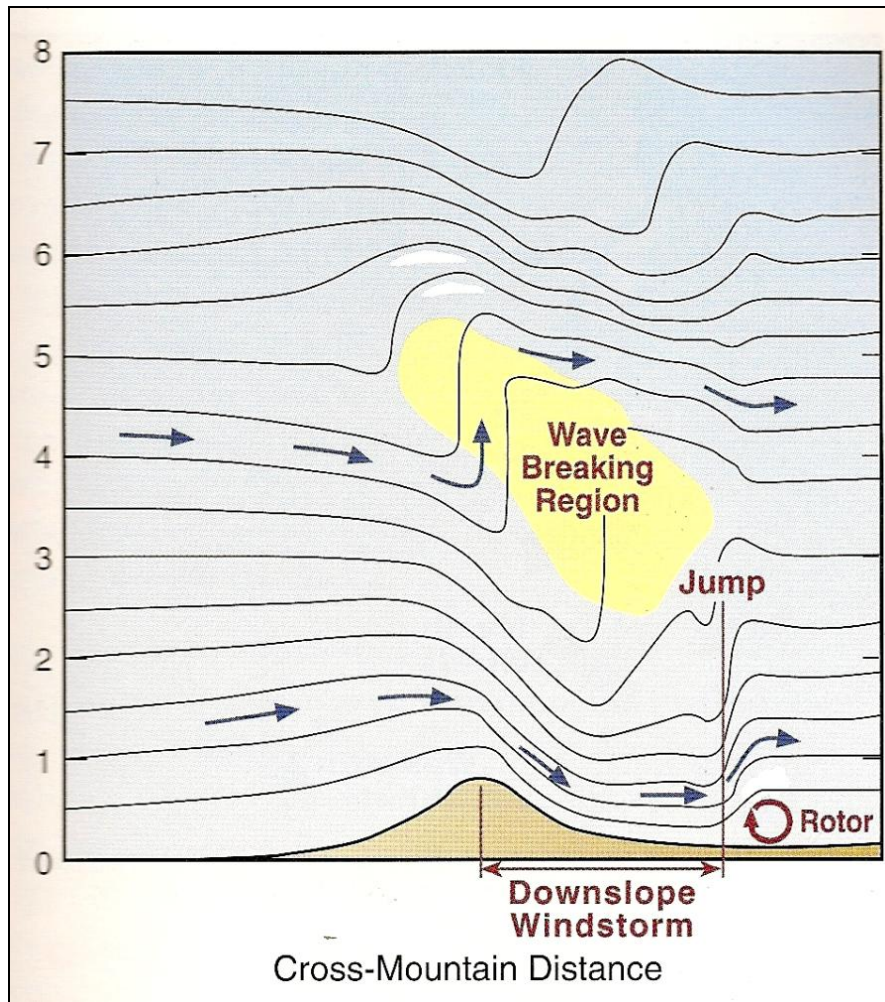


**Figure 24 – Cross section of a mountain wave**

The characteristics of mountain waves in conjunction with downslope windstorms in the vicinity of Boulder, Colorado, have been intensively studied since the early 1970s<sup>18</sup>. Aircraft measurements taken during the Boulder windstorm on January 11, 1972, where show that the severe downslope windstorm was a surface manifestation of a large amplitude wave extending up to 40,000 feet (figure 25 (Lilly 1978)). Numerous regions of turbulence were encountered by the research aircraft at upper levels, as well as below 15,000 ft, including near both Denver Stapleton and Jefferson County airports. There are also several crests of lee waves in the stable layer extending downstream of the jump region. In this case, the turbulence was encountered underneath these lee waves, above and to the east of Denver Stapleton airport.

<sup>18</sup> Klemp, J. B., and D. K. Lilly, 1975: The dynamics of wave-induced downslope winds. *Journal of Atmospheric Science*, 32, 320-339.

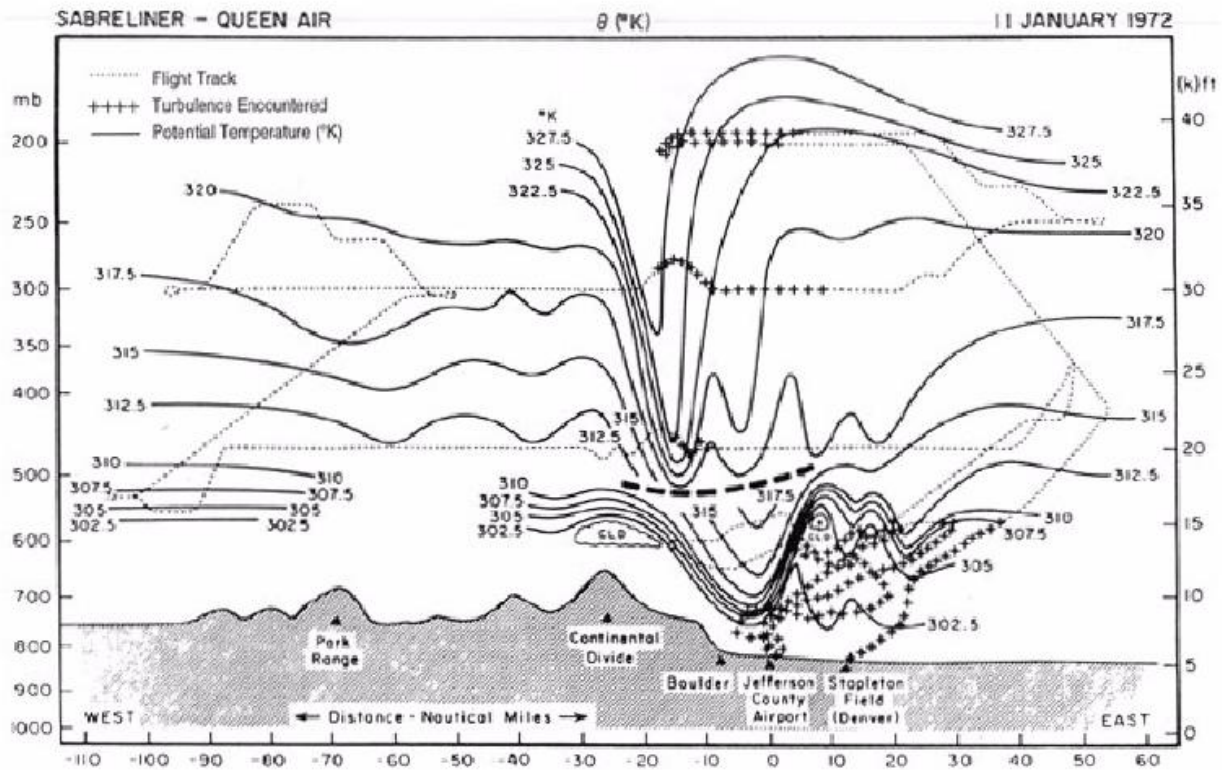


**Figure 25 – Analysis of aircraft measurements of the atmosphere taken during the January 11, 1972 windstorm (from Lilly 1978). Lines of potential temperature are in solid lines, aircraft tracks in dashed lines with “+” marks indicating where the aircraft reported encountering significant turbulence.**

Studies focusing on the violent windstorms in and around Boulder have found the strength, location and timing of the maximum surface wind speeds varies greatly, depending on the structure of the atmospheric flow impinging on the Rockies<sup>19</sup>, as well as characteristics of the air mass to the east<sup>20</sup>. Some wind events are confined to a narrow region close to the foothills, while others occur over a wide region along the Front Range. A climatological study<sup>21</sup> of sounding features favoring Boulder windstorms include the existence of a stable layer with relatively strong westerly/northwesterly flow near mountain top, with little directional change or strong vertical

<sup>19</sup> Mercer, A.E., M.B. Richman, H.B. Bluestein, and J.M. Brown, 2008: Statistical Modeling of Downslope Windstorms in Boulder, Colorado. *Weather and Forecasting*, 23, 1176–1194, and Durran, D. R., 1986: Another look at downslope windstorms. Part I: The development of analogs to supercritical flow in an infinitely deep continuously stratified fluid. *Journal of Atmospheric Science*, 43, 2527-2543.

<sup>20</sup> Lee, T. J., R. A. Pielke, R. C. Kessler, and J. Weaver, 1989: Influence of cold pools downstream of mountain barriers on downslope winds and flushing. *Monthly Weather Review*, 117, 2041-2058.

<sup>21</sup> Brinkmann, W. A. R., 1974: Strong downslope winds at Boulder, Colorado. *Monthly Weather Review*, 102, 592–602.

wind shear through the troposphere. Numerous observational, theoretical and numerical studies since then have explored the conditions conducive to, and mechanisms involved in, strong windstorm development. Though exact mechanisms of windstorm development continue to be an area of active research, most studies have confirmed the stable layer near ridge top level combined with a strong cross-mountain (westerly) flow component are key atmospheric conditions favoring windstorms. These conditions existed on the day of the accident.

Also of importance to the KDEN accident is the fact that propagating wind gusts have been observed in association with windstorm events. Using Doppler lidar Neiman et al. (1988)<sup>22</sup> measured coherent, eastward propagating wind gusts with periods of 4-5 minutes and 14 minutes during a January 1987 windstorm near Boulder. These resulted in wind speeds varying from around 22 to 36 m/s (44 to 72 knots) within about 5 km (16,000 feet). The source of the surface gustiness has been investigated using numerical models<sup>23</sup>. In simulations of the January 9, 1989, windstorm some of gustiness appears to arise from large amplitude lee waves downstream of the main wave breaking region<sup>24</sup>.

While severe windstorm events are relatively infrequent, mountain wave activity over the Rocky Mountains is quite common. Pilot reports of mountain waves and turbulence occur regularly in the absence of strong surface winds. Thus the effects of mountain waves, even large amplitude turbulence generating waves, may not always penetrate to the surface. Of particular concern to aviation are situations in which large amplitude waves intermittently erode to the surface, generating transient high speed wind gusts. Model results (section 7) indicate intermittent penetration of large amplitude lee waves may have resulted in periods of strong wind gusts at KDEN.

Visual indicators of mountain wave activity, such as lenticular clouds, also occur regularly in the winter time in Colorado. Dr. John Brown, from NOAA in Boulder (personal communication) has observed intermittent periods of moderate wind gusts associated with cloud patterns indicative of a large amplitude mountain wave over the foothills combined with several lee wave crests extending downstream, similar to the model results for KDEN. His observations suggest these conditions occur on the order of 20 times per year during the winter months. Note, however, this is probably an underestimate, since these waves may occur under conditions in which no clouds are formed to mark their existence.

---

<sup>22</sup> Neiman, P. J., R. M. Hardesty, M. A. Shapiro, and R. E. Cupp, 1988: Doppler lidar observations of a downslope windstorm. *Monthly Weather Review*, 116, 2265-2275.

<sup>23</sup> Peltier, W. R. and T. L. Clark, 1979: The evolution and stability of finite-amplitude mountain waves. Part II: Surface wave drag and severe downslope windstorms. *J. Atmos. Sci.*, 36, 1498-1529, and Peltier, W. R. and J.F. Scinocca, 1990: The Origin of Severe Downslope Windstorm Pulsations. *Journal of Atmospheric Science*, 47, 2853-2870.

<sup>24</sup> Clark, T. L., W.D. Hall, and R.M. Banta, 1994: Two- and Three-Dimensional Simulations of the 9 January 1989 Severe Boulder Windstorm: Comparison with Observations. *Journal of Atmospheric Science*, 51, 2317-2343.



Much of the research on mountain waves in Colorado have focused on severe windstorm events, due to the damaging nature of these storms combined with the high density of atmospheric scientists in the Boulder area. However, more moderate mountain wave wind events that may be associated with intermittent gustiness, especially further east over the Denver area, have not been as well studied. Because of this there is little climatological guidance regarding the magnitude and frequency of mountain wave related windstorm events or periods of moderate gustiness at KDEN.

### **6.0.2 Mountain wave conditions 20 December 2008**

Synoptic conditions showed strong westerly to northwesterly flow, combined with a stable layer above mountain top, over the Rocky Mountains at the time of the accident. These conditions are conducive to mountain wave activity. However, as mentioned in Section 1.0.3, several conditions were different from the “typical” Boulder strong downslope windstorm. In particular, the vertical shear was higher than in previous documented climatology study of Boulder windstorms. Also, the surface pattern, with a high to the northeast of Colorado (Figure 9), was not typical for a “classic” strong downslope windstorm event in Boulder.

Nonetheless, a number of factors point to mountain waves as a contributing factor in the gustiness and turbulence along the Front Range of the Rockies at the time of the accident. Specifically,

- Many mountain wave and turbulence pilot reports were reported on that day, indicating mountain wave activity and turbulence due to breaking mountain waves.
- There is an indication of a large scale hydrostatic mountain wave in RUC analysis.
- Persistent feature in satellite imagery through out the day indicating region of clearing possibly due to subsidence associated with mountain wave.
- Strong upper-level flow across mountain range.
- The presence of a stable layer above mountain top.
- Strong gustiness observed in the LLWAS and WSSDM data at KDEN.
- Temperature rise associated with wind speed gusts in WSSDM data.

To further understand the cause of the gustiness at KDEN, a high resolution, multi-nested nonhydrostatic model, with a horizontal resolution of 250 m was used to simulate conditions on that day. Results show a large amplitude lee wave associated with intermittent strong winds penetrating to the surface over KDEN. These model results are presented and discussed in the next section.

## 7.0 NCAR Simulations of Meteorological Conditions

To assess whether mountain waves could have played a role in the gustiness at KDEN NCAR ran a high resolution numerical model to simulate conditions surrounding the period.

### 7.0.1 Numerical Model

The multi-nested parallelized version of the Clark-Hall anelastic terrain-following mesoscale model was used to simulate the three-dimensional flow conditions affecting KDEN at the time of the accident. Dr.'s William Hall, Teddie Keller and Robert Sharman contributed to the execution and analysis of the model for this case.

The Clark-Hall (C-H) model<sup>25</sup> has demonstrated success in simulating mountain waves and downslope windstorms in research mode. A number of studies have compared Clark-Hall model output to observations, providing ample evidence of the model's ability to reproduce observations. Examples include successfully reproducing the observed features surrounding mountain wave events, as well as simulating meteorological conditions associated with aircraft turbulence encounters. This model has also been used to investigate the mechanisms involved in gustiness associated with downslope windstorms<sup>26</sup>. Thus this model should be ideally suited for simulating conditions associated with this accident. It should be noted, however, that mesoscale models in general cannot be expected to reproduce the exact timing and intensity of observed wind gusts and turbulent patches due to problems associated with such effects as initialization uncertainties and oversimplified sub-grid scale turbulence parameterizations.

The C-H model was initialized using output from the RUC model at 1500 MST on December 20, 2008, and hourly RUC data provided boundary conditions as the model was integrated in time. Thus only information from observations assimilated through the RUC model were included in the C-H model run, i.e. LLWAS and WSSDM data were not incorporated. The model utilized five progressively higher resolution nested domains, allowing for increasing resolution both horizontally and vertically in the area of interest. The following table lists the grid size, horizontal resolution, and starting time for each domain. DX and DY are the horizontal grid spacing, NX, NY, and NZ are the number of grid points in the east-west and north-south, and vertical directions. Higher resolution nested domains were added to the simulation at the times indicated, it should also be noted that these higher resolution nested domains include more data than

---

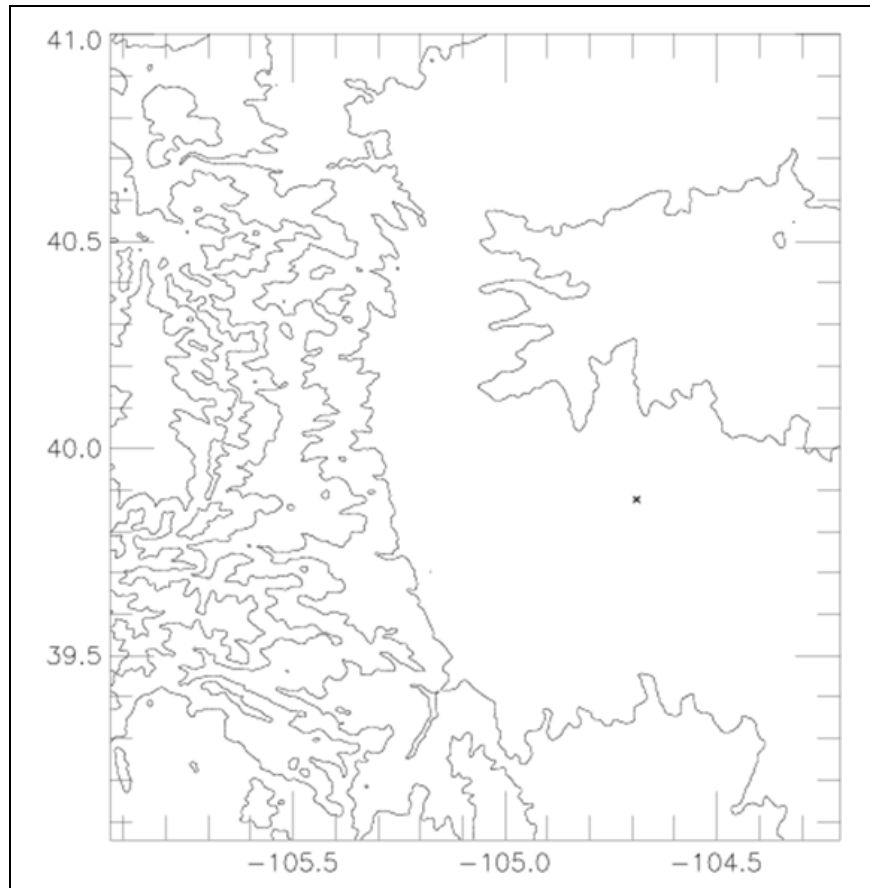
<sup>25</sup> Clark, T. L., 1977: A small scale dynamic model using terrain-following coordinate transformation. *J. Comput. Phys.*, 24, 186–215; Clark, T. L. and R. Gall, 1982: Three-dimensional numerical model simulations of air flow over mountainous terrain: A comparison with observation. *Monthly Weather Review*, 110, 766–791; and Clark, T. L. and W.D. Hall, 1996: The Design of Smooth, Conservative Vertical Grids for Interactive Grid Nesting with Stretching. *Monthly Weather Review*, 35, 1040–1046.

<sup>26</sup> Clark, T. L., W.D. Hall, and R.M. Banta, 1994: Two- and Three-Dimensional Simulations of the 9 January 1989 Severe Boulder Windstorm: Comparison with Observations. *Journal of Atmospheric Science*, 51, 2317–2343.

operational numerical weather prediction models, such as the RUC. This allows for much shorter wavelength gravity waves and mesoscale eddies to be resolved by the model.

Domain	DX, DY	NX	NY	NZ	Domain Started
1	18 km	130	194	81	1500 MST (2200Z)
2	6 km	194	290	140	1500 MST (2200Z)
3	3 km	194	290	134	1600 MST (2300Z)
4	1 km	290	434	128	1700 MST (0000Z)
5	0.25 km	587	866	122	1730 MST (0030Z)

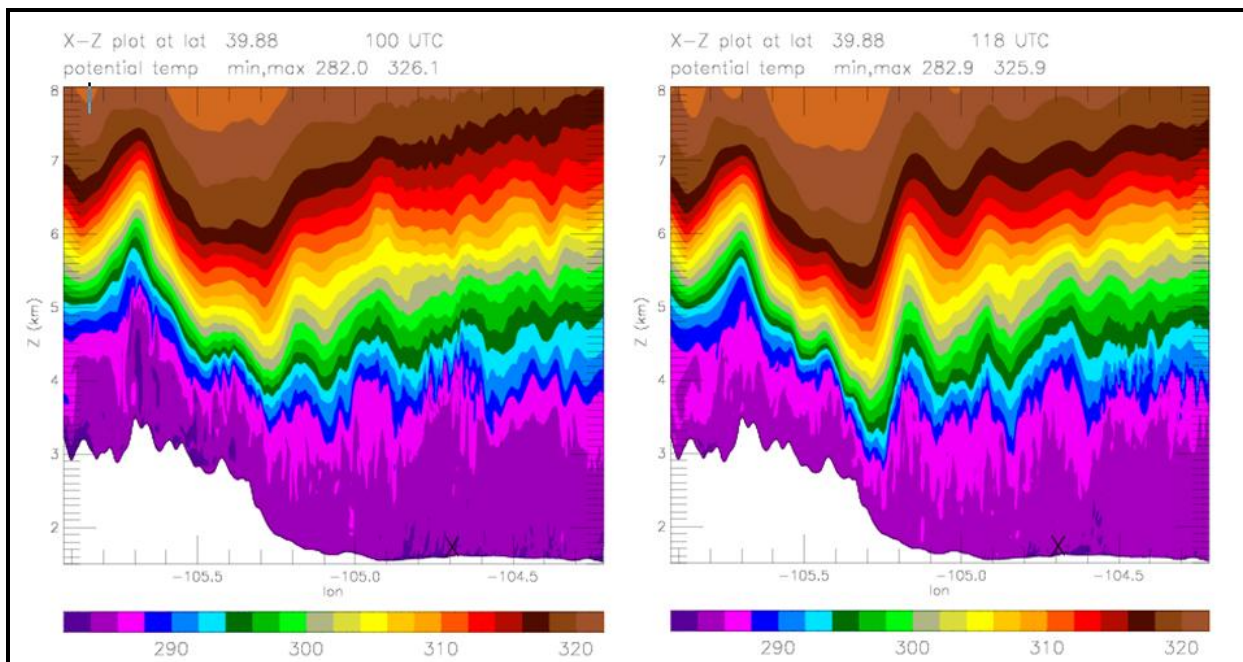
Figure 26 shows the topography and extent of the inner most, 250 meter horizontal resolution, domain.



**Figure 26 – Topography from the model in domain 5. Contour interval is 500 meters. KDEN is marked by the X.**

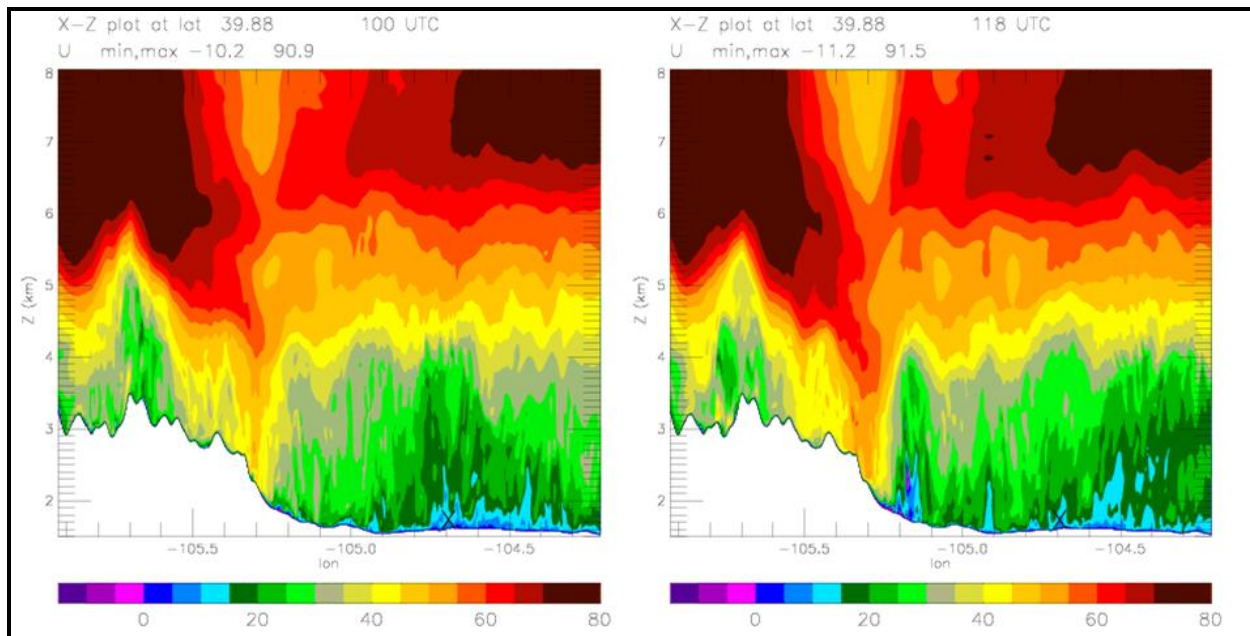
## 7.0.2 Numerical Simulation Results

Results from the Clark-Hall model simulation indicate significant mountain wave activity over the Rocky Mountains during the time of the accident. Figure 27 is a vertical cross section through the inner domain of the model at the latitude of KDEN at 1800 and 1818 MST, and depicts a well defined wave over the mountains, with the wave trough extending downward above the foothills to the west of KDEN. Although the position of the dominant wave trough did not change much during the hour surrounding the accident, the amplitude of the wave increased significantly shortly before accident. In addition to the large wave over the mountains a train of partially trapped lee waves extends downstream along the elevated stable layer, indicated by the series of wave crests over KDEN. These lee waves have a wavelength of approximately 20-25 km. Associated with the undulations of these lee waves are fingers of warmer air extending downward into the boundary layer below.



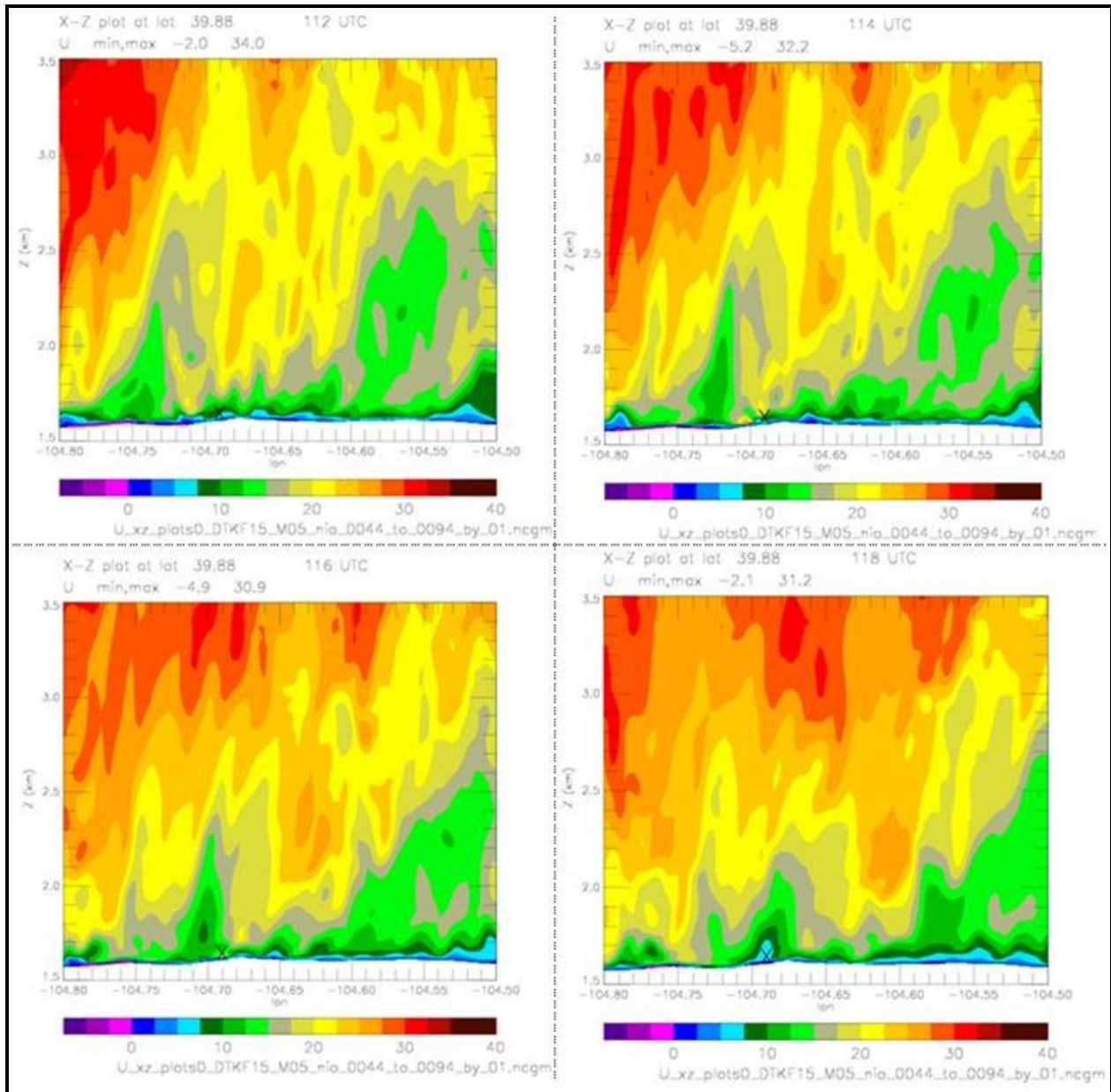
**Figure 27 – Potential temperature along a vertical slice in the inner model domain for 1800 and 1818 MST (0100Z and 0118Z) respectively.**

Figure 28 is a plot of the east-west wind velocity (U component) for the same vertical cross section and depicts a region of high velocity air extending downward in association with the wave over the mountains. Over the higher elevation slope west of KDEN winds of 40 to 50 m/s (approximately 80 to 100 knots) were depicted. The U component wind speeds along the slope of foothills increase near the time of the accident, and there is a region of reversed (easterly) flow just above the base of the foothills, indicated by the pink colors. Downstream near KDEN wind speeds below the stable layer varied with undulations in the lee waves aloft.



**Figure 28 – Contours of the east-to-west (U) component of the wind for 1800 and 1818 MST respectively. Contours are at 5 m/s. Pink colors indicate negative contours or easterly flow.**

Figure 29 focuses in on the region directly above KDEN and revealed a more complex spatial and temporal variability in the U wind speed. Note that the U wind component represents a cross wind for the north-south runways at KDEN. Fingers of high velocity penetrating downward below the lee waves in the stable layer create velocity increases from about 5 to 20 m/s (10 to 40 knots) over a 4 minute period at KDEN in this particular cross section.



**Figure 29 – Contours of the east-to-west U component of the wind focused in on the area near KDEN. Top of the plot is 3.5 km or approximately 12,000 feet msl. Times are at 1812, 1814, 1816 and 1818 MST.**

Horizontal plots of the east-west velocity U at 14.7 m agl (approximately 48 feet agl) in the area immediately surrounding KDEN from 1804 through 1818 MST (0104Z-0118Z) are shown in figures 30 and 31. Also plotted are both model (black) and LLWAS (red) wind vectors. The LLWAS winds have been converted from magnetic to true north to compare with model winds.

These images depict generally stronger westerly flow to the north of the airport, with large regions of relatively lighter winds over the center and southern portions of the airport. There are

patches to the south of the airport where the U component is negative (easterly), designed in pink. Note the generally good agreement between the LLWAS and model winds, which bolsters the confidence in the model predictions.

Embedded in the overall flow structure are many gusts which move from west to east across the domain. For example, a particularly strong gust with east-west wind speeds reaching more than 35 m/s (68 knots) can be seen propagating across the southern end of the airport during the 10 minute time period from 1808 to 1818 MST. As it moves across the airport it tracks just south of runway 7/25, then over the approach end of runways 35L and 35R. It should be noted that there had been wind shear alerts for runway 7 within minutes of the accident.

Another gust with east-west wind speeds over 20 m/s (40 knots) moves over runways 34L and 34R, directly crossing the accident site, between 1814 and 1816 MST. This represents a 40 knot cross-wind gust.

In summary, the NCAR model shows a large amplitude lee wave extending downstream of the mountains over KDEN. Regions of high velocity extend downward from this wave. Pulsations in the lee wave amplitude are manifested at the surface as intermittent gustiness.

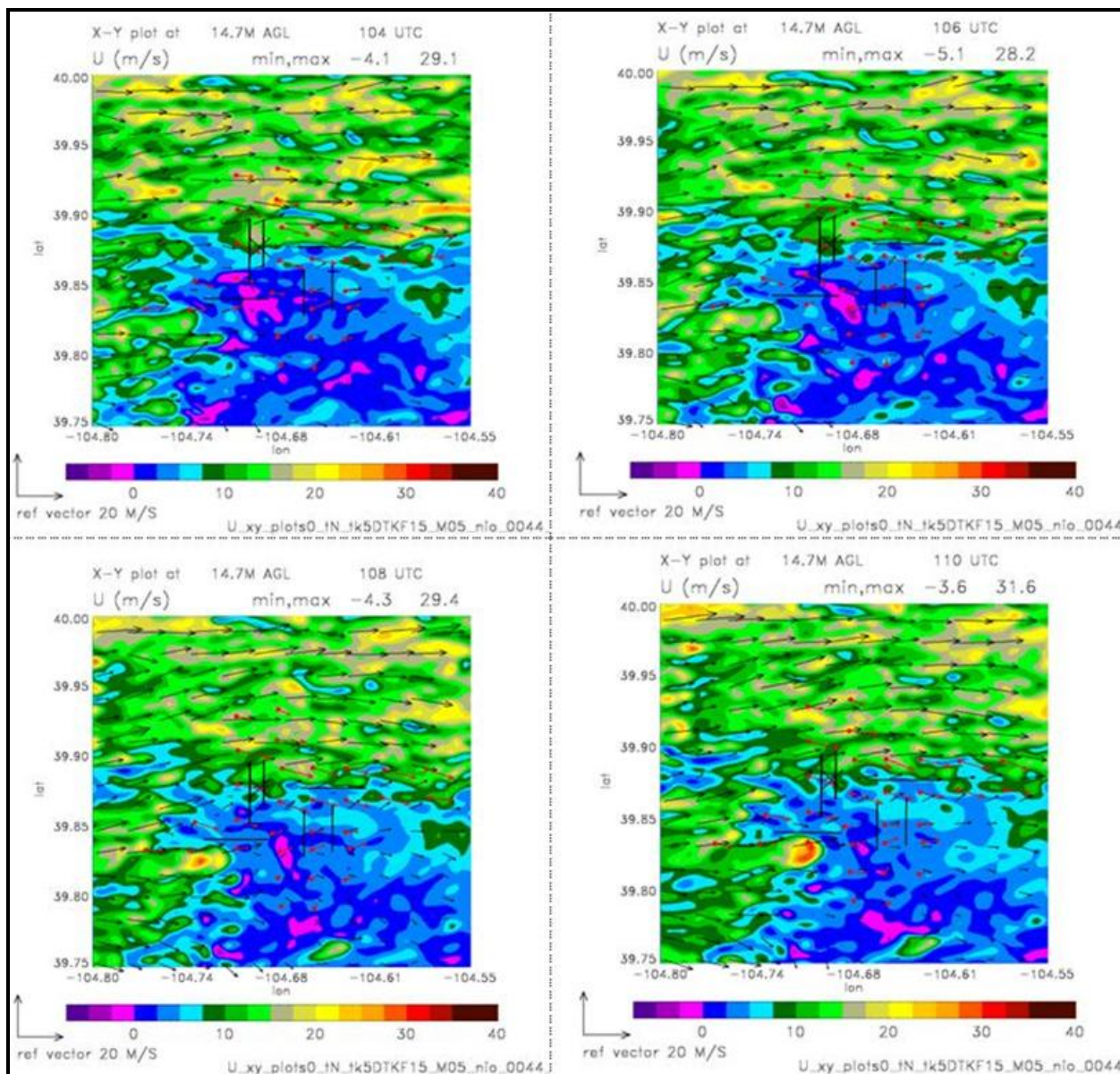
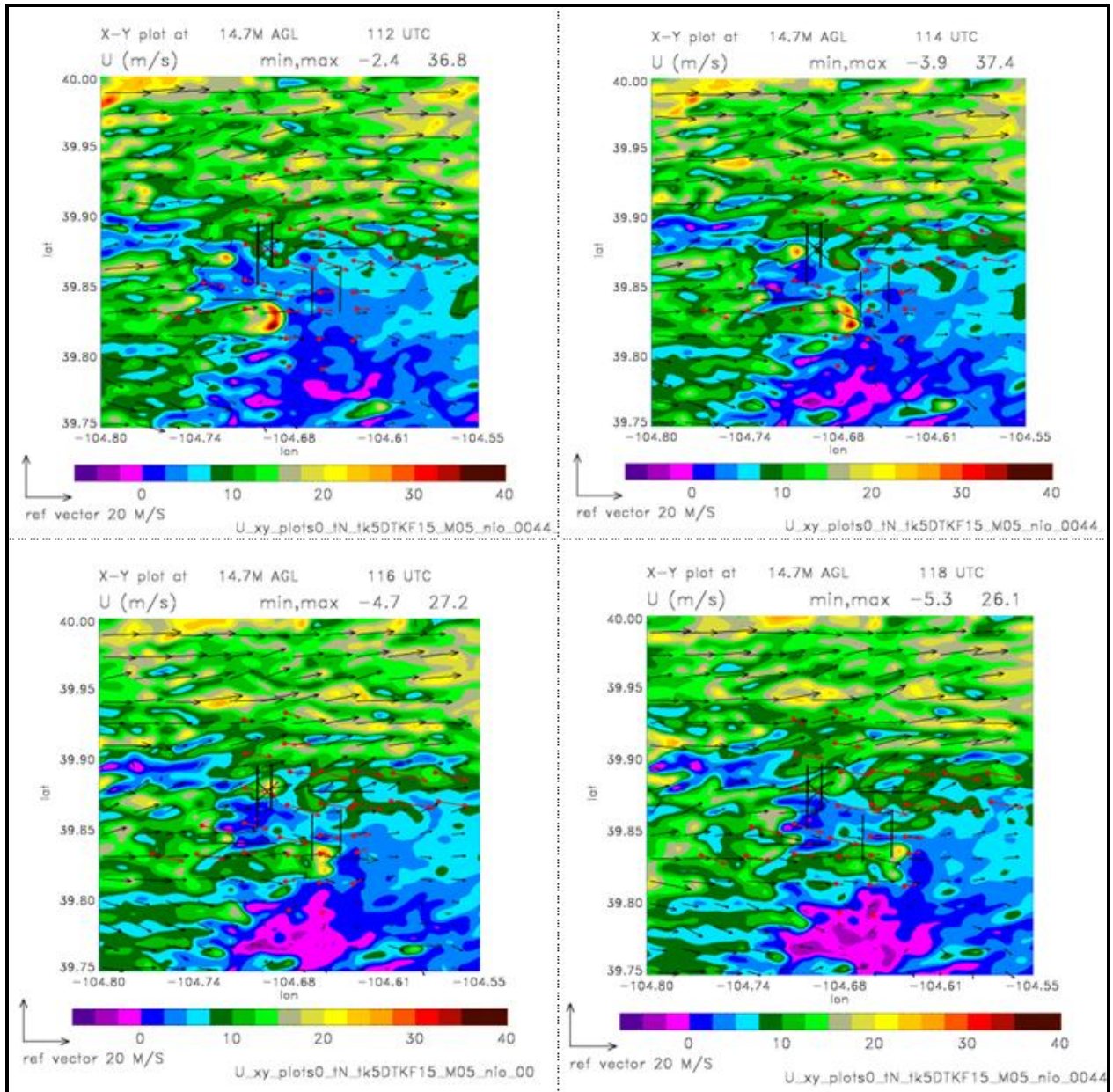


Figure 30 – Horizontal plots of the east-to-west velocity  $U$  at 14.7 m (48 ft) agl for the area surrounding KDEN at 1804, 1806, 1808, and 1810 MST. Runways are marked by black lines. The black arrows represent model winds and the red arrows the LLWAS winds converted from magnetic to true direction. Pink areas are negative or easterly flow.





**Figure 31– Same as figure 28, except times are 1812, 1814, 1816, and 1818 MST.**

## 8.0 Pilot Reports

The following pilot reports (PIREPs) were recorded over Colorado between 1500 and 2300 MST on December 20, 2008. The reports are in standard format and code, and are as follows:

TAD UA /OV 80 E CIM/TM 2203/FL380/TP B757/TB MDT/RM MDT MTN WAVE FL370B380 +/- 20 KTS  
 ZAB=  
 ASE UA /OV DBL 080050/TM 2240/FL400/TP CL60/RM MOD MTN WAVE +/-200 FT..ZDV=  
 DEN UA /OV DEN /TM 2254 /FL400 /TP C550 /TA M25 /WV 29283KT /TB OCNL LGT CHOP=  
 APA UA / OV APA /TM 2255 /FL080 /TP BE35 /TB MOD /RM STRONG MT WAVE=  
 ALS UA / OV CIM020020/TM 2256/FL370/TP A319/TB MDT MTN WAVE/RM + - 15 KTS=  
 ALS UA / OV CIM010020/TM 2256/FL470/TP LJ45/TB MDT MTN WAVE/RM -+ 15 KTS ZAB=  
 BKF UA / OV DEN215010 /TM 2300 /FL001 /TP B737 /TB MOD BLO 180=  
 TAD UA / OV TBE/TM 2310/FL360/TP A320/TB MOD/RM ZDV =  
 BKF UA / OV APA350007 /TM 2355 /FL090 /TP C550 /TB LGT-MOD=  
 BJC UA / OV DEN270025 /TM 0000 /FL090 /TP B737 /TB MOD 090-170=  
 DEN UUA/ OV FQF 306050/TM 0025/FLDURD/TP DH8B/TB MOD-SEV FL180-170/RM ZDV =  
 DEN UA / OV DVV 220060/TM 0041/FL160/TP LJ35/TB MOD/RM ZDV =  
 BJC UUA / OV BJC045001/TM 0059/FL059/TP LJ35/RM LLWS -10KT SPD VARN FROM BJC ATCT=  
 MTJ UA /OV MTJ 030035/TM 0100/FLDURD/TP PA31/TB MOD AOB 170/RM RPRTD BY SVRL  
 ACFT..ZDV=  
 BJC UA / OV DEN270025 /TM 0108 /FL170 /TP B737 /TB MOD 170/BLO /RM DURC DENA=  
 GUC UA / OV HBU 260026/TM 0110/FL380/TP A319/RM MTN WAVE +/-500 FT +/-M .02..ZDV=  
 DEN UUA / OV FQF 306055/TM 0115/FLDURD/TP LJ25/TB SEV-EXTREME FL190-170/RM OCNL MOD  
 AOB 170..ZDV=  
 FNL UUA / OV DEN325050 /TM 0118 /FL190 /TP LJ25 /TB SEV-EXTRM /RM DENA=  
 GUC UA / OV HBU/TM 0135/FL350/TP A320/TB CONT MOD CHOP/RM ZDV =  
 FCS UA / OV COS135015 /TM 0156 /FL110 /TP MD81 /TB LGT OCNL MOD /RM COSA=  
 FNL UA / OV DEN325040 /TM 0241 /FL130 /TP DH8D /TB MOD /RM DENT=  
 GXL UA / OV DEN360020 /TM 0241 /FL160 /TP B737 /TB LGT-MOD 140-160 /RM DURC DENT=  
 ALS UA / OV ALS 135035/TM 0325/FLDURD/TP BE58/RM SEV MTN WAVE FL180-170..ZDV=

The reports confirmed turbulent conditions over Colorado associated with mountain wave activity, which was described as moderate to severe by several pilots with airspeed variations of +/- 15 knots and 500 feet altitude deviations. There were also two reports of pilots encountering severe to extreme turbulence, which is defined as the aircraft is impossible to control and might have caused structural damage. In addition, there were also several reports of low-level wind shear (LLWS) during the period.

## 9.0 Center Weather Service Unit Products

The Denver (KZDV) Air Route Traffic Control Center (ARTCC) Center Weather Service Unit (CWSU) normal hours of operation was from 0600 to 2200 local. A search of the NWS database indicated that the KZDV issued no Meteorological Impact Statements (MIS) or Center Weather Advisories (CWA) during the period.

## 10.0 WSSDM Surface Data at KDEN

Data from two surface stations, identified as sensor DIA1 and DIA2, were located at KDEN as part of the NCAR's Weather Support to Deicing Decision Making (WSDDM) program<sup>27</sup> provided temperature and relative humidity information in addition to wind data. DIA1, located at, was near LLWAS station 2 (latitude 39.870 N, and longitude 104.679 W). The sensor is mounted at a height of 10 feet (3 meters). The sensor at DIA2, mounted on a 32 foot tower (10 meters) was located west of the southern end of runway 34L (latitude 39.855 N, longitude 104.718 W)<sup>28</sup>.

Figure 32 shows wind speed and gusts, wind direction, temperature and relative humidity for the period 1700 through 1900 MST on December 20, 2008 (0000Z through 0200Z on December 21, 2008) for DIA1. Prior to 1750 MST (0050Z) temperatures slowly decreased (sunset occurred at 1639 MST). Temperatures then rose slightly after 1750 MST, when winds speeds began to increase. During the twenty minute period surrounding the time of the accident, from approximately 1810 to 1830 MST, there was a rapid jump in both wind speed and gustiness. Note increases in temperature coincided with the wind speed bursts. The wind direction was approximately constant throughout this period, and relative humidity decreased when wind speeds, gustiness and temperature increased. Similar plots for DIA2 are shown in figure 33.

---

<sup>27</sup> See [www.rap.ucar.edu/projects/wsddm](http://www.rap.ucar.edu/projects/wsddm)

<sup>28</sup> More information on the two sites can be found at [www.rap.ucar.edu/projects/winter/sites/DIA1](http://www.rap.ucar.edu/projects/winter/sites/DIA1) and [www.rap.ucar.edu/projects/winter/sites/DIA2](http://www.rap.ucar.edu/projects/winter/sites/DIA2).

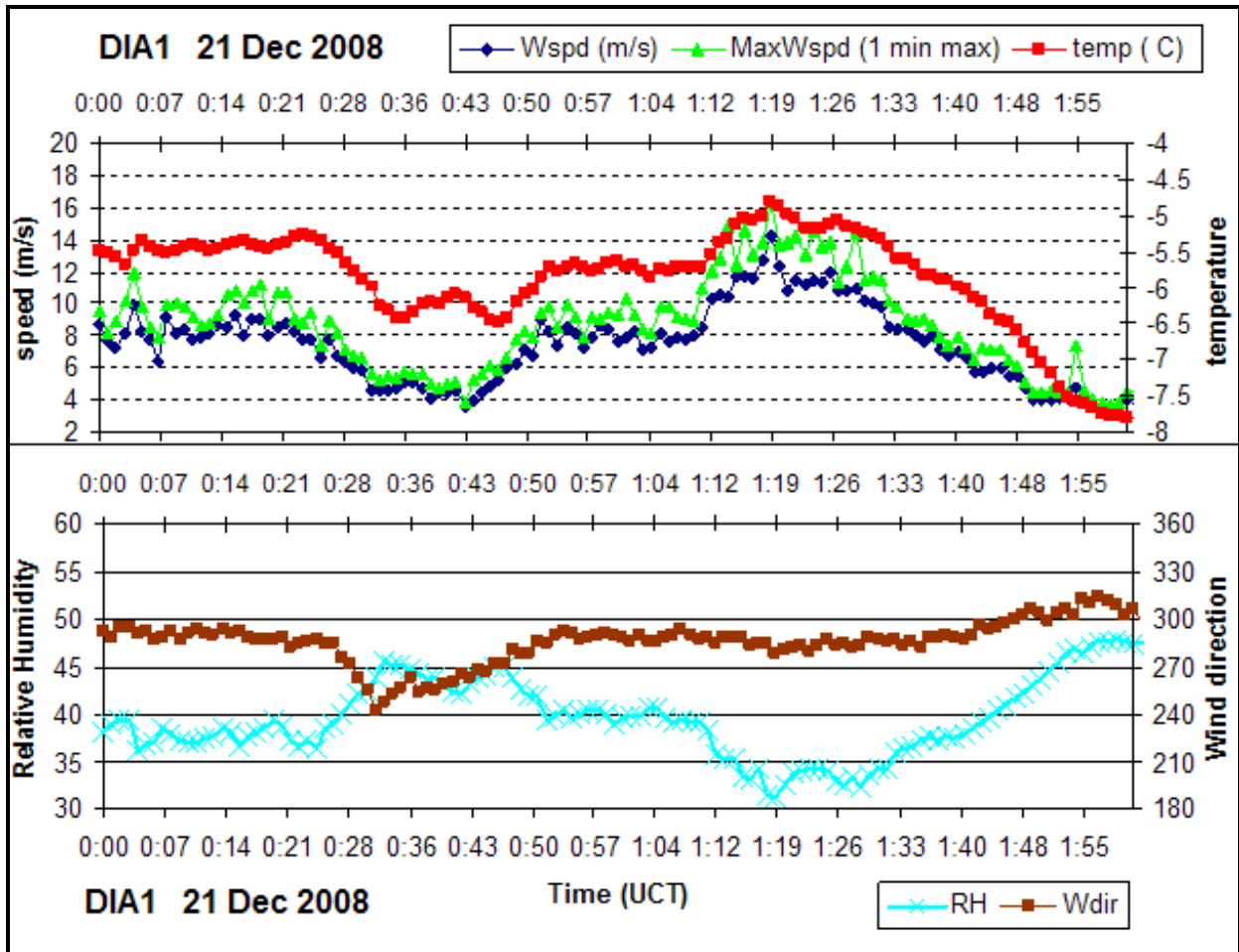


Figure 32 - DIA1 data (a) Wind speed (m/s) (blue), maximum wind gusts (green), and temperature (°C) (red) for the time period 1700 – 1900 MST (0000Z – 0200Z). (b) Wind direction (brown) and relative humidity (light blue) for the same time period.

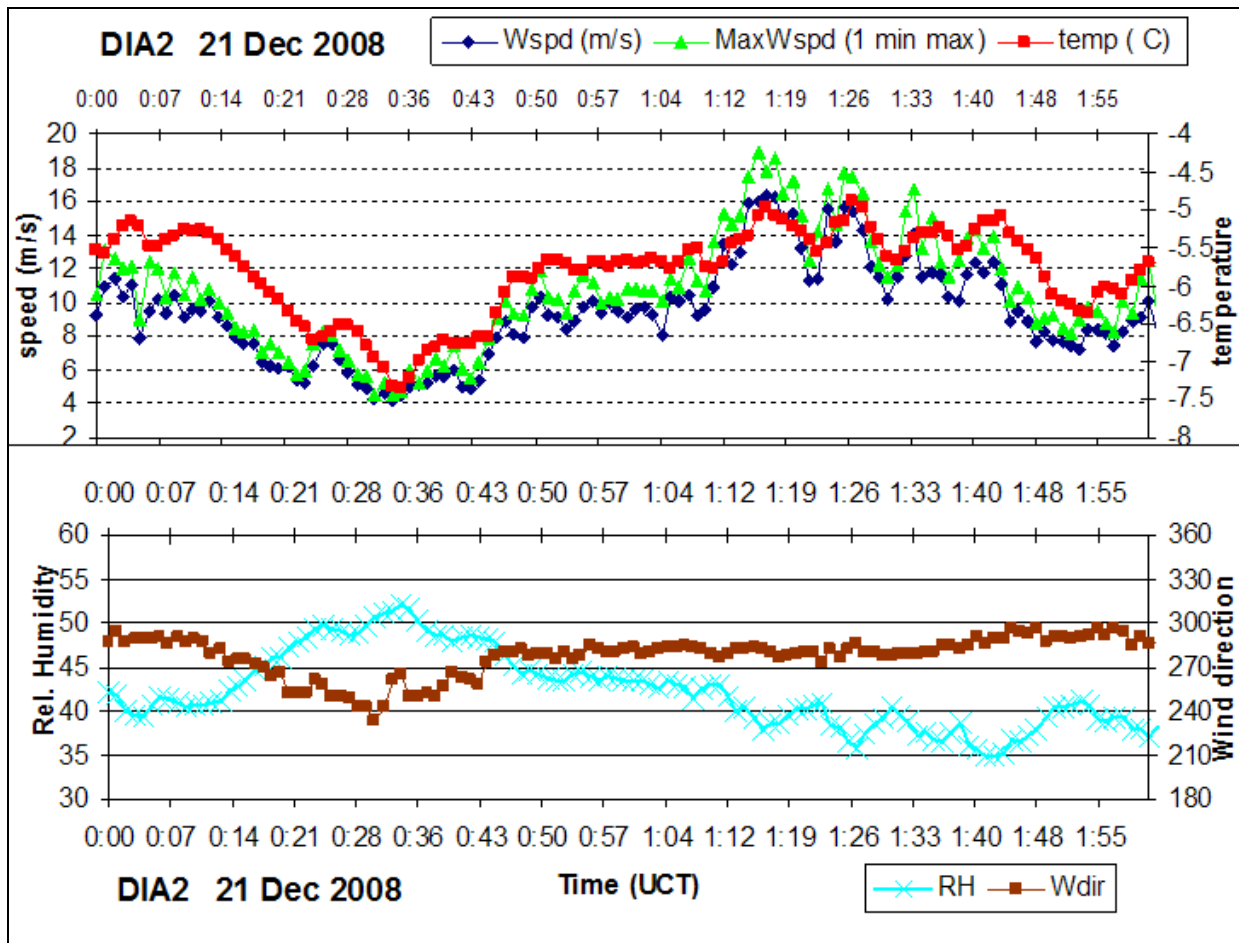


Figure 33 – same as figure 29 for DIA2 data

### 11.0 Other Wind Measurements

Although Boulder did not experience a significant windstorm on the day of the accident, there were moderate gusts above 40 mph in the area as reported by Dr. John Brown, of NCAR. Dr. Brown keeps a personal record of winds in the Boulder area, from measurements taken at NCAR in Boulder (Mesa and Foothills Laboratories, [www.eol.ucar.edu/cgi-bin/weather.cgi](http://www.eol.ucar.edu/cgi-bin/weather.cgi)) as well as at the National Renewable Energy Lab south of Boulder (NREL; [www.nrel.gov/midc/nwtc\\_m2](http://www.nrel.gov/midc/nwtc_m2)), noting time periods with gusts above 40 mph. In the 3 hour period from 1700 to 2000 MST on December 20, 2008 (0000Z to 0300Z December 21, 2008) the largest gust, 55 mph (47.8 knots), occurred at the Mesa Lab site. Also, in the 12 hour period ending 2000 MST, both NREL and NCAR’s Foothills lab experienced maximum gusts of 45 mph (39 knots) and 44 mph (38 knots), respectively. This is in contrast to the 48 hours following 0200 MST (0900Z) on December 21, 2008, during which none of these stations experienced gusts above 40 mph.

It is important to note that these wind measurements do not address whether or not there may have been strong downslope winds along the slope of the mountain foothills west of Boulder.

Donald E. Eick  
NTSB Senior Meteorologist